Working Paper No.262

An approach to characterizing the water content of soils by thermal infrared remote sensing.

M.D. ELKINGTON

School of Geography
University of Leeds

December 1979.

ABSTRACT

Several existing techniques for relating remotely sensed data from aircraft and spacecraft to soil moisture are reviewed. An approach for characterising the moisture content of a cropped surface by remote sensing, based upon a simulation model of the soil-plant-atmosphere continuum is presented and discussed. The data requirements of this approach are supplied by routine meteorological measurements, remote sensing and one-time field measurements of certain parameters. Simulation results from the model are presented and give good agreement with measured values. The implementation of this approach in studies utilising satellite and aircraft remote sensing is discussed in the context of the Heat Capacity Mapping Mission and the recent aircraft experiments in Europe.

C O N T E N T S

1. *INTRODUCTION*

There is a need for integrative measures of land and water potential which are capable of being applied broadly over large areas and which can provide periodically a generalised knowledge of distributions of major earth resources. The need for such measures exists in the many disciplines concerned with earth resources but is particularly urgent in those disciplines which are concerned with the study of renewable earth resources. One such resource is water, a highly variable and mobile resource, which has been the focus of geographical interest for many years.

Information about the moisture content of soils is required for investigation in many different fields of geographical research. It is particularly important for investigations in agriculture where the quantity of water in the soil has a direct influence on the efficient and sustained production of crops. It is also important for many other types of investigation such as studies in hydrology and meteorology. There are therefore many different fields in which information about the distribution of soil moisture is required.

Information about the moisture content of soils is generally required at frequent intervals so that changes in moisture content can be monitored and compared with the incidence of rainfall, the rate of crop growth, the volume of ground water run-off or the occurrence of earthflows and related geomorphological phenomena. Presently this information is collected manually by traditional methods of field inspection and sampling. The limitations of these manual methods of monitoring soil moisture have become more apparent in recent years however as more detailed information is required from larger areas (Webster, 1977)). The major limitations are:

(i) that the precision of the information is not as great as is often needed because of the low density of sampling points and the long interpolations required;

(ii) that many classes of information of importance such as pockets of saturated soil are not collected at all;

(iii) that the degree of timeliness of the decisions based on the information about soil moisture is becoming more inadequate (Holter *et al.*, *1970*). For these reasons it is becoming increasingly important to develop other means of collecting information about the distribution of soil moisture.

There are today several new and promising ways of collecting information about the moisture content of soils. Amongst these for example is the neutron probe, an instrument based upon the principle of neutron absorption. Given an adequate density of such instruments in an area information may be collected automatically, but the precision of the information will still be determined largely by the sampling density and procedures for interpolation. Nevertheless these methods do offer the prospect of substantially improving existing methods based upon routine field inspection and sampling by teams of soil surveyors.

Much more promising in the long term is the prospect of determining the moisture content of soils by remote sensing from aircraft and earth orbital satellites. Studies by Moore et al *(1975)* and Idso et al *(1975)* have shown that it is possible to correlate emitted and reflected radiation, measured by remote sensors with measurements of soil moisture content. There is a need however for a physically based technique that is capable of calculating soil moisture contents from measurements of some variable that can be obtained using a remote sensor. One such variable is surface temperature, which can be measured with a high accuracy using a line scanning radiometer sensitive to radiation in the infra-red part of the spectrum.

The temperature of a fallow soil or a vegetative surface is an integral response by that surface to environmental factors such as the level of incoming radiation, the temperature and humidity of the air and the wind velocity. Several characteristics of that surface such as the albedo, the aerodynamic roughness and the moisture content alter the effect of environmental factors in the energy budget and heat exchange at that surface. These characteristics may therefore be reflected in the thermal response of that surface. Thus, by determining the effect of variations in the moisture content on the diurnal course of the surface temperature it will be possible to determine the moisture content from remotely sensed measurements of the surface temperature.

The Heat Capacity Mapping Mission (HCMM) launched in April *1978* is an earth orbital satellite that determines the surface temperature by measuring the emitted radiation from the surface in the 8μm - 14μm waveband. Several workers in Europe and the U.S.A are assessing the

feasibility of using such satellite data for soil moisture surveys. In addition the Joint Flight Experiments in Germany and Britain which took place in the Summer of *1979* involved the use of a multispectral scanner in an aircraft to investigate the distribution of soil moisture at a smaller scale than information provided by the satellite.

The basic problem to be solved before remote sensing of soil moisture from aircraft and spacecraft becomes feasible on a routine basis is how to relate the temperature data supplied by the remote sensor to the soil moisture on the ground. The aim of this paper will accordingly be:

(i) to review the various techniques which have been suggested for relating the remotely sensed data to the degree of soil moisture on the ground;

(ii) to describe the rationale and theory of a new approach to characterising the moisture content of a soil by remote sensing from aircraft and spacecraft;

(iii) to discuss the scope and limitations of the new approach and recommend how it may be implemented for studies with the HCMM and aircraft data.

2. REVIEW

The amount of water stored near the terrain surface is of considerable significance from both theoretical and practical viewpoints. Soil moisture is a basic component in the hydrologic cycle, in energy exchange near the surface, and in modelling various ecosystem processes. From a practical viewpoint, knowledge of soil moisture levels is important for growing crops, flood forecasting and wildlife management. The present approach to estimating soil moisture content is based on a real extrapolation of point measurements. This extrapolation is questionable since the distribution of soil moisture varies spatially (Dawdy et al. *1969;* Huff, *1966*).

An alternative approach is to estimate soil moisture by remote sensing methods which can directly cover large areas within a short time period. Qualitative and quantitative measurements of remotely determined soil moisture have been attempted using different regions of the spectrum (Tanguay,*1969;* Myers and Heilman, *1969;* Edgerton, *1972;* Ulaby et al, *1973)*

Remote sensors utilise electromagnetic radiation (EMR) from micro-waves to visible waves collected from the land, water and atmosphere. The EMR in travelling from its initial source to the remote sensor undergoes absorption, re-radiation, reflection, scattering, polarization and spectral redistribution. The changes in the EMR from source to sensor can be subtle or pronounced, depending upon the interactions that take place with the media or materials involved. These changes can supply the user with information about temperature, moisture, texture and electrical properties of whatever has been surveyed (fig *2(a)*).

According to Sellers (*1965*), approximately *30%* of the solar radiation reaching the outer boundary of the earth's atmosphere is reflected and scattered back into space by clouds, aerosols and other atmospheric constituents. Approximately *17%* of the incoming radiation is absorbed by the earth's atmosphere and about *22%* reaches the earth's surface as diffuse radiation. Only about *31%* of the radiation entering the outer boundary of the earth's atmosphere therefore reaches the surface as direct solar radiation (fig *2(a)*).

Incoming radiation received at the earth's surface is either absorbed, reflected or transmitted. Remote monitoring of reflected or emitted radiation will therefore provide information about the energy absorption characteristics of a surface. The absorption of energy into

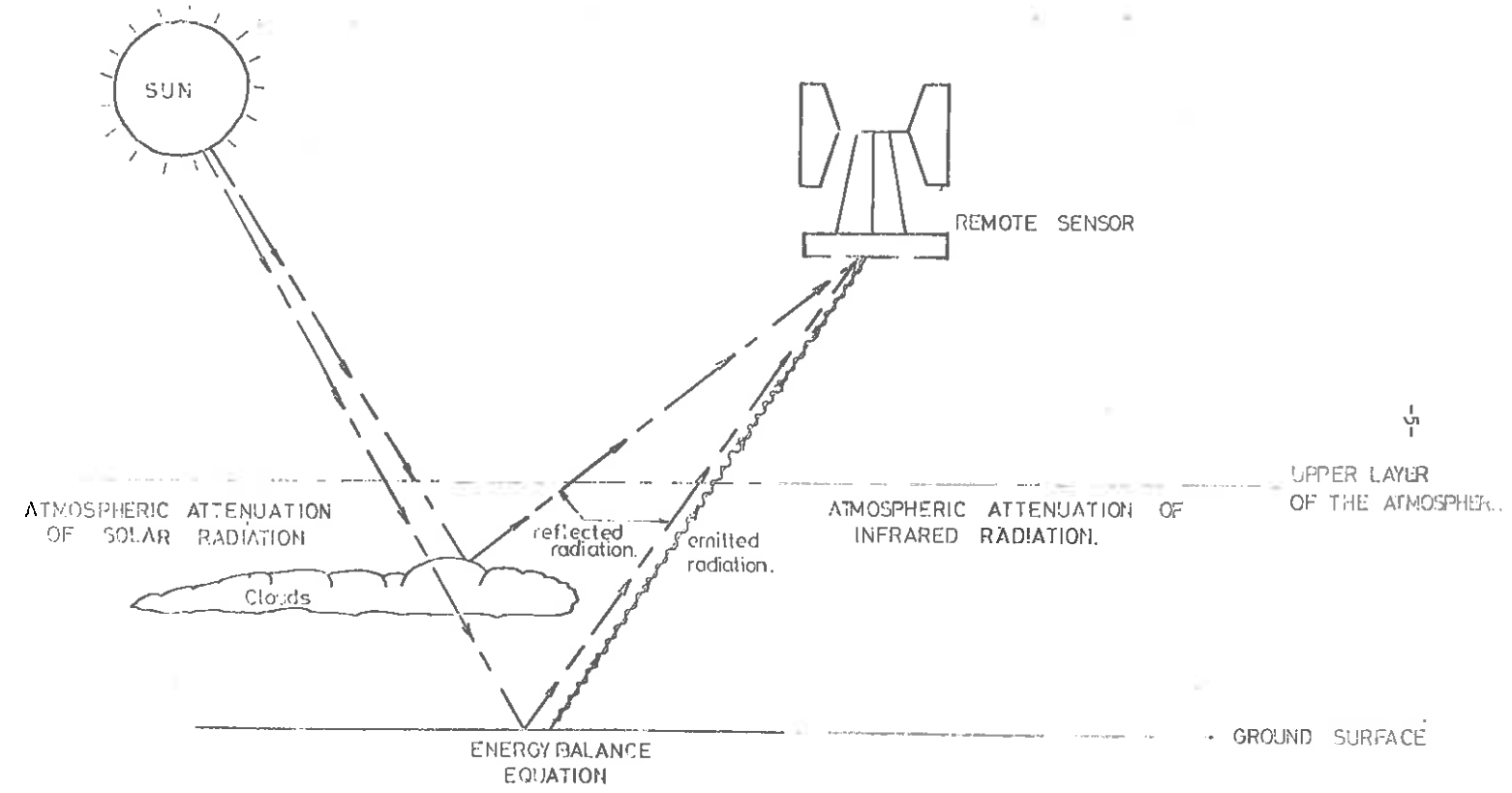

Fig (a): A SIMPLE MODEL OF THE INTERACTION OF ELECTROMAGNETIC RADIATION WITH THE ATMOSPHERE.

a crop canopy or soil is dependent on a number of factors, one of which is the moisture content of the soil. It is therefore possible to study soil moisture using remotely sensed measurements of reflected and emitted radiation.

Quantitative measurements of remotely determined soil moisture have been attempted using different regions of the spectrum; visible, near-infrared, thermal infrared and microwave (Tanguay, *1969;* Werner and Schmer, *1971;* Allen, *1972;* Parks et al, *1973;* and Schmugge et al, *1974*). Schmugge et al (*1974*) demonstrated that microwave radiometers are sensitive to the moisture content of the top few centimetres of a soil profile. The application of such radiometers is however limited by their relatively coarse spatial resolution. This review will therefore concern itself with remote sensing of soil moisture using shorter wavelengths in the visible and infrared (*0.4*µm to *14.0*µm region).

Two methods for estimating soil moisture remotely using the *0.4*µm to *14.0*µm wavelength region are: (1) measurement of spectral reflectance, and, (2) measurement of soil temperature. The reflectance method is based on observations showing that directional reflectance decreases as soil moisture increases for a given soil. The soil temperature method is based on observations of emitted radiation showing that differences between the diurnal maximum and minimum soil temperatures decrease as the moisture content increases for a given soil.

1) Reflectance Method (reflected radiation)

Directional reflectance measurements performed by Blanchard et al (*1974*) revealed that the reflectance of a soil decreases as soil moisture increases, for wavelengths from *0.4* to *1.3* microns. This observation is valid for any soil type but it can be applied only for a given soil at any one time, because the reflectance value is affected by different grain sizes, textures and mineralogy. Recent studies (Parks et al, *1973*) show that this relationship may continue to a wavelength of *2.5*µm but so little solar radiation of this wavelength reaches the ground that this relationship may not be helpful for field studies.

Idso et al (*1975*) has shown that albedo is a good descriptor of surface soil moisture content. Two major disadvantages restrict the application of this technique, however. Firstly the correlation of

reflectance measurements with deep soil moisture contents (below *10*cms from the surface) is poor for light applications of water. Secondly, the albedo's of different soils differ so greatly that there is little hope that a universal relation requiring no ground truth can be derived using this parameter (Idso & Reginato, *1974*).

Werner and Schmer (*1972*) investigated the application of remote sensing techniques to the inventory of soilmoisture in croplands and rangelands. Data from several film-filter combinations within the reflective region were collected. They concluded that the blue region of electromagnetic spectrum could be used for determining soil water conditions with little or no crop cover. The green, red and near infrared regions were all useful for evaluating soilmoisture where crop or range canopies were present.

The reflectance differences among crop types are considerable and varied with phenological stage; (Werner and Schmer, *1972;* Allen, *1972)* therefore, the reflective spectral region has limited use for predicting moisture variation within diverse agricultural regions. Since water has a considerable affect on the energy budget, surface emittance variations may provide a better estimate of soil moisture as it is less influenced by crop cover.

2) Temperature Method (emitted radiation)

Initial attempts to correlate soil temperature with soil moisture were qualitative. These studies (Myers and Heilman, *1969)* revealed that temperature differences occured between wet and dry areas of a given soil. In general, during the day, the wet soil was cooler than the dry soil, and during the night the wet soil was warmer than the dry soil.

Research by Jackson et al *(1973)* and Idso et al *(1975)* indicates that the difference between maximum and minimum soil temperatures taken over a diurnal cycle decreases with increasing soil moisture. This correlation (fig *2(b)*) is valid for soil layers to a depth of *10*cm and is probably valid for soil depths equaling the solar heating influence during the diurnal cycle (approximately *50*cm).

As the moisture content increases in the soil (by displacing air in the intergranular pore spaces), the bulk density (ρ), specific heat (c), and thermal conductivity (k) also increase. Soil moisture affects each of

DIURNAL TEMPERATURE VARIATION VS SOIL MOISTURE

(after Jackson, 1973)

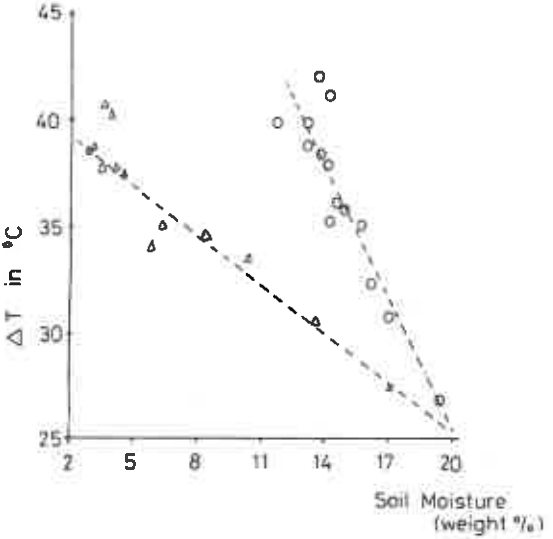

△ 0 – 1 cm layer.

o 5 – 9 cm layer.

FIG. 2(b)

these parameters and it is therefore necessary to relate them to some other parameter that is a measure of p, c and k. Thermal inertia ($\sqrt{k.p.c}$) or thermal diffusivity ($k/p.c$) are two possible parameters. Thermal inertia is a measure of the rate of heat transfer at the interface between two dis-similar madia (e.g. soil and air) whereas thermal diffusivity is a measure of the change in temperature produced in a substance as heat flows through it (e.g soil at different depths). For all soils, thermal diffusivity increases more rapidly than thermal inertia as moisture content increases (Nakshabondi and Kohnke, *1965*).

For the soil moisture - temperature correlation to be valid, both maximum and minimum soil temperatures must be known. Maximum and Minimum soil temperatures can be derived however if soil temperatures are measured near the diurnal extremes of heating and cooling with a calibrated infrared radiometer. The thermal inertia or thermal diffusivity of that same soil must also be measured. The temperature and thermal data can then be used in a radiative heat-transfer model (Watson, *1971*) to calculate ground temperature versus time over a diurnal cycle for materials of different thermal properties. In addition to calculating temperature versus time for materials having different thermal inertias, this model provides corrections for site latitude, slope directions, slope angle, solar declination and albedo. Using only a one-time measurement of thermal properties, a radiative heat-transfer model and periodic day and night remotely sensed temperature values, seasonal changes in fallow soil measure can be assessed to a depth of approximately *10*cm.

Correlative studies at the US DA Water Conservation Laboratory has shown that the volumetric water content of the surface soil layer was a linear function of the amplitude of the diurnal surface soil temperature wave.(Idso et al, *1975*). The moisture content of the soil was also found to be a linear function of the daily maximum value of the surface soil-air temperature differential. The above functions were tested initially on bare soil but were later applied to cropped surfaces with some success. (Idso and Eshler, *1976*).

The approaches to the remote sensing of soil moisture described above indicate the feasibility of monitoring soil moisture by remote sensing. They do not however solve the problem of providing a quantitative estimate of the soil moisture content of a vegetated surface. Most of the research to date has been concerned with estimation of the soil moisture content

from large homogenous areas of fallow soil. The effect of including a layer of vegetation is a complex one and not easily quantified. A method that incorporates remotely sensed parameters in a physically based model of the soil - plant - atmospheric continuum (SPAC) may provide a solution to this problem.

A number of SPAC models of varying complexity have been developed in the last two decades. A review by Phillips (*1966*) details the history of this type of model.

Many of the more recent models (Goudriaan J. & P. E. Waggoner, *1972*; Waggoner et al *1969*) are too complex to be of use in a remote sensing system. The TERGRA model however was developed by Soer (*1977*) as an aid for the interpretation of thermal infrared images of cropped surfaces. The TERGRA model simulates the thermal behaviour of cropped surfaces and is based on the transport equations of one dimensional vertical heat and moisture flow from the soil through the plant to the atmosphere. The model is broadly analogous to an electrical resistance model, with the transport equations having driving forces and resistances. The use of the TERGRA model in a remote sensing system is restricted by the need for a number of ground based measurements.

This paper describes a model developed for a remote sensing system that is capable of predicting the soil moisture content of a cropped surface. It is the intention that all data input to the model should be supplied by remote measurements, one time measurement of ground properties and routine meteorological measurements.

3. BACKGROUND

3.1 The energy balance over a short crop

The balance of energy at the surface of a short crop may be represented in terms of various energy fluxes:

$$Rn + G + H + L.E = 0 \qquad (1)$$

where Rn = Net radiation flux ($W.m^{-2}$)

G = Ground heat flux ($W.m^{-2}$)

H = Sensible heat flux ($W.m^{-2}$)

L = Latent heat of vapourisation ($J.kg^{-1}$)

E = Evapotranspiration flux ($kg.m^{-2}.s^{-1}$)

Each element in equation 1 is a function of the temperature of the crop. The temperature of the crop can therefore be estimated by using an iterative technique to balance this equation.

The flux direction of the energy balance components are dependent on time of day and climatic conditions. During the day, radiation from the sun is absorbed by the soil and the crop. Thus, the soil and crop surfaces become warmer than the air so that the sensible heat flux is upward away from these surfaces. During the day under stable conditions, the soil surface is warmer than the soil at greater depths so that the soil heat flux is downward away from the crop. At night, soil and crop surfaces lose heat through the emission of longwave radiation; therefore, heat flux in the soil is toward the crop to counteract the radiation loss. At night, the air is normally cooler than the crop resulting in sensible heat flux away from the crop volume.

If water is available for evaporation, the latent heat flux is upward away from the crop volume during the day. At night, the latent heat flux may be away or toward the crop volume depending on the respective temperatures of the air, crop, and soil surfaces. In regions with dry climates, latent heat flux will normally continue to be away from the crop both day and night and dew formation will not occur. When the crop temperature is less than the dew point temperature however, the latent Heat flux will be toward the crop canopy

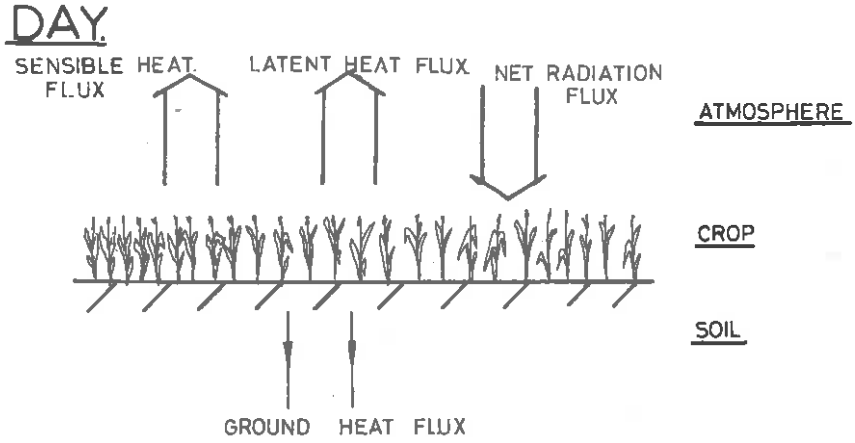

FIGURE 3(a)

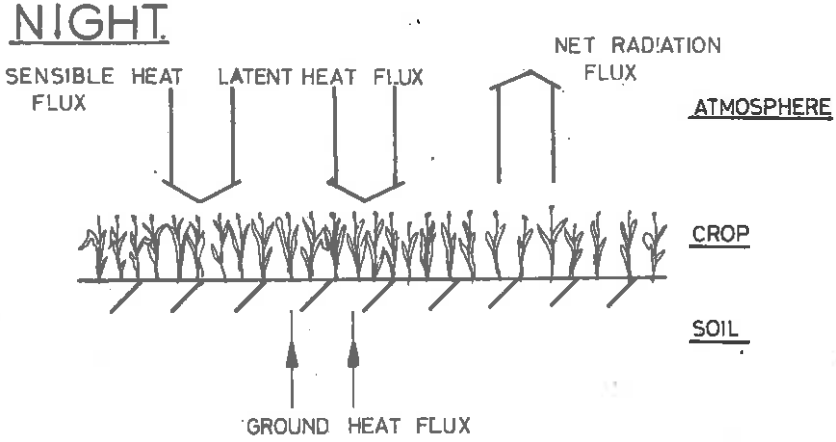

FIGURE 3(b)

and dew formation will occur. Figures 3a and 3b show the directions of the energy fluxes for a typical short crop during the day and night.

Many different sign conventions are used in the literature on the energy balance of crops and there seems to be little agreement between workers in different fields. The sign convention followed in this paper is that fluxes are positive when they are directed toward the surface of the crop and negative when they are directed away from the surface of the crop.

Equation 1 is a simplified form of the energy balance equation. It takes no account of the energy used by the crop for photosynthesis or of the changes in the heat storage of the crop. The equation is frequently used in this form however over short crops where the effects of these factors are relatively small (Moore et al (1975)).

3.2 Net Radiation Flux

The net radiation flux (Rn) is the sum of the incoming and outgoing components of radiation and may be expressed as follows:

$$Rn = (1 - \alpha_s) R_s + (1 - \alpha_L) R_L - \varepsilon \sigma T_c^4 \qquad (2)$$

Net Shortwave Radiation	Net Longwave Radiation (Sky)	Emitted Longwave Radiation

Rn = net radiation flux ($W.m^{-2}$)

α_s = crop reflection coefficient for shortwave radiation

α_L = crop reflection coefficient for longwave radiation

R_s = incoming shortwave radiation ($W.m^{-2}$)

R_L = incoming longwave radiation ($W.m^{-2}$)

ε = crop emission coefficient

σ = Stefan Boltzmann constant ($\sigma = 5.67 \times 10^{-8}$ $W.m^{-2} k^{-4}$)

T_c = crop temperature (k)

Since:

$$(1 - \alpha_L) = \varepsilon$$

equation (2) can be rewritten as:

$$R_n = (1 - \alpha_s) R_s + \varepsilon(R_L - \sigma T^4) \qquad (3)$$

Measurements of net radiation should preferably be used in this model, but as the majority of meteorological stations do not routinely record net radiation or any of its components the net radiation in this study is calculated from estimates for the values on the right hand side of equation (3).

3.2.1 Shortwave Radiation Flux R_s

It is possible to simulate R_s for a diurnal period if values for the sun's declination and the cloud cover at a given point are known. For example, one method of calculating R_s uses at atmospheric transmission coefficient, which is given in tables(Smithsonian Meteorological Tables, ed List, R. J. (1968)). Another method has been used however that does not require reference to tables, provides more accurate results and is easier to use in a computer model (Gadd and Keers, (1970)). This method uses the following equation:

$$R_s = R_o.(0.6 + 0.2\ (\mathrm{Sin}\ \beta\ )).\ \mathrm{Sin}\ \beta\ .\ C_k \qquad (4)$$

where R_o = solar constant ($W.m^{-2}$)

β = solar elevation (^{o})

C_k = cloud factor

The solar elevation is calculated using a subroutine called SUNELP. The cloud factor (C_k) is expressed in terms of the cloud fractions at high (C_H), medium (C_m) and low (C_L) levels:

$$C_k = (1.0 - 0.4\ C_H).\ (1.0 - 0.7\ C_m)\ .\ (1.0 - 0.7\ C_L) \qquad (5)$$

3.2.2 Coefficient of Shortwave Reflection (α_s)

There are a number of empirical relationships for estimating albedo (Kalma and Badham (1972)). A relationship established by Ross (1975) is used in this model:-

$$s = \frac{m}{1 + b\ \mathrm{Sin}\ (\beta)}$$

where α_s = shortwave reflection coefficient

α_m = dummy reflection coefficient for $\beta = 0$

β = solar elevation (^{0})

b = a constant dependent on the crop structure.

This relationship produces values for the albedo that give good agreement with results published by Ahmad (1978) and Monteith (1959). Research by Soër (1977) has shown that this relationship works well for grass when α_m is fixed at 0.33 and b is 0.6. Further research into the value of the constant for crop structure is required if the model is to be applied to cereal crops.

3.2.3 Longwave Sky Radiation

The value for the longwave sky radiation in the net radiation equation is the most difficult to estimate accurately. This is because clouds have a complex effect on longwave sky radiation.

Brunt (1939) showed that the value of the longwave sky radiation for cloud-free conditions is a function of the temperature and humidity of the air:

$$R_L = \sigma T_a^4 (a + b\sqrt{e_a}) \qquad (7)$$

where R_L = longwave sky radiation ($w.m^{-2}$)

T_a = air temperature (K)

σ = Stefan-Bolzman constant

e_a = water vapour pressure in the air (Pa)

a and b are empirically derived values.

A linear regression of measurements of R_L on measurements of T_a and e_a gave valuesof 0.526 and 0.0065 for a and b respectively.

Under cloudly conditions Brunt's relationship has to be modified by a function given by Gadd and Keers (1970):

$$R_L = T_a(a + b.e_a).(1.0 - 0.1C_H - 0.3C_m - 0.6C_L) \qquad (8)$$

A comparison of the values estimated using the above relationship and measurements of longwave sky radiation generally showed good agreement.

3.2.4 Emission Coefficient

There is little information in the literature on how the emission coefficient varies with crop structure. For the purpose of this study the emission coefficient was fixed at 0.95 because this value has been used extensively by other workers (Soer, 1977). The effect of the emission coefficient on the energy balance has been investigated using this model and the results are presented in section 5.1.6.

3.3 Sensible Heat Flux

The sensible heat flux above a crop can be expressed in the form of a transport equation as follows:

$$H = \rho C_p \frac{T_a - T_c}{r_a} \qquad (9)$$

where T_a = air temperature (K)

T_c = crop temperature (K)

H = sensible heat flux ($w.m^{-2}$)

ρ = density of moist air ($Kg.m^{-3}$)

C_p = specific heat per unit mass of air ($J.Kg^{-1}.K^{-1}$)

r_a = turbulent diffusion resistance for heat and water vapour transport ($s.m^{-1}$)

The turbulent diffusion resistance r_a is a function of the wind velocity, the stability of the atmosphere just above the crop, and the nature of the crop surface. In this model the turbulent diffusion resistance is calculated according to three conditions of stability.

(i) Neutral Stability ($T_c = T_a$)

The model is programmed to have neutral stability when the crop temperature is within 0.2^0K of the air temperature. Under these conditions the expression used to calculate the turbulent diffusion resistance is as follows:

$$r_a = \frac{\ln\left(\frac{z_a - d}{z_{om}}\right).\ln\left(\frac{z_a - d}{z_{oh}}\right)}{K^2 u} \qquad (10)$$

where u = wind velocity ($m.s^{-1}$)

K = von Karmans constant (0.4)

z_a = reference level in the atmosphere (m)

d = zero plane displacement (m)

z_{om} = crop roughness length for momentum (m)

z_{oh} = crop roughness length for sensible heat (m)

The roughness length for momentum z_{om} and the roughness length for sensible heat z_{oh} are calculated assuming:

$$z_{oh} = z_{om} = z_o \qquad (11)$$

where z_o is the crop roughness (m) and is derived from the height of the crop using a simple relation established by Monteith (1973):

$$z_o = 0.13h \qquad (12)$$

where h = crop height (m).

Recent work by Thom (1972) has shown that z_{oh} is an order of magnitude lower than z_{om} and that it depends not only on the nature of the surface but on the nature of the surrounding air. As there seems to be little experimental evidence in the literature and no other suitable relationship, equation (11) will be used in this model.

(ii) Unstable Conditions ($T_c > T_a$)

If evapotranspiration from a crop is reduced due to the closure of leaf stomata, the temperature of a crop will rise and unstable conditions will occur. Under such conditions, Paulson (1971) has shown that r_a can be expressed as follows:

$$r_a = \frac{\left|\ln\left(\frac{z_a - d}{z_{om}}\right) - P_1\right| \cdot \left|\ln\left(\frac{z_a - d}{z_{oh}}\right) - P_2\right|}{K^2 u} \qquad (13)$$

where P_1 and P_2 are functions of the Monin-Obukhov length. Thus:

$$P_1 = 2\ln\left(\frac{1+x}{2}\right) + \ln\left(\frac{1+x^2}{2}\right) - 2\arctan(x) + \frac{\pi}{2} \qquad (14)$$

$$P_2 = 2\ln\left(\frac{1+x^2}{2}\right) \qquad (15)$$

where

$$x = \left(1 - 16\,\frac{z_a - d}{A}\right)^{0.25} \qquad (16)$$

and A = Monin-Obukhov length (m).

Several workers have derived semi-empirical formulae for mass and heat transport above a crop using the Monin-Obukhov length as a measure for stability (Monin and Obukhov, 1954; Businger, 1966; Dyer 1967).

$$A = \frac{u_*^3 \rho C_p T_a}{KgH} \qquad (17)$$

where u_* = friction velocity ($m.s^{-1}$)

g = acceleration due to gravity ($m.s^{-2}$)

K = von Karman's constant

H = sensible heat flux ($w.m^{-2}$)

ρ = density of moist air ($Kg.m^{-3}$)

C_p = specific heat per unit mass of air ($J.Kg^{-1}.K^{-1}$)

T_a = air temperature (K)

Soër (1977) has suggested a simplification that enables the Monin-Obukhov length to be estimated without using an iterative technique. If equation (11) is assumed, the Monin-Obukhov length can be found approximately from the following relationship:

$$\Lambda \approx \frac{T_a . u^2}{g(T_a - T_c)} \cdot \frac{1}{\ln(\frac{z_{a-d}}{z_o})} \qquad (18)$$

for $\Lambda < -1.5$m with a maximum error in r_a of about 1%.

(iii) Stable Conditions ($T_a > T_c$)

For stable conditions the formulae established by Webb (1970) may be used with the value of the constant in this relationship being fixed at 4.7 as suggested by Businger, et al. (1971).

$$r_a = \frac{\left|\ln(\frac{z_{a-d}}{z_{om}}) + 4.7\,\frac{z_{a-d}}{\Lambda}\right| . \left|\ln(\frac{z_{a-d}}{z_{oh}}) + 4.7\,\frac{z_{a-d}}{\Lambda}\right|}{K^2 u} \quad \text{for } \Lambda > z_{a-d} \qquad (19)$$

$$r_a = \frac{\left|\ln(\frac{z_{a-d}}{z_{om}}) + 4.7\right| . \left|\ln(\frac{z_{a-d}}{z_{oh}}) + 4.7\right|}{K^2 u} \quad 0 < \Lambda < z_{a-d} \qquad (20)$$

The above relations for r_a are only approximate but they appear to work well unless the wind velocity above the crop is below 0.5 $m.s^{-1}$. To prevent the formulae becoming unstable at low wind velocities a lower limit of 0.5 $m.s^{-1}$ is used in the model.

3.4 The Evapotranspiration Flux

This component of the energy balance equation can be estimated in many ways. Many simulation models estimate a value for the latent heat flux which is equal and opposite to the sum of the other three parameters in the energy balance equation (eg. Ripley, et al., 1973). The model described in the study however, uses the transport equation described by Soër (1977):

$$L.E. = \frac{\rho C_p}{\gamma} \cdot \frac{e_a - e_c^*}{r_a + r_c} \qquad (21)$$

where γ = psychrometric constant ($Pa.K^{-1}$)

e_c^* = saturated water vapour pressure in the air at temperature T_c (Pa)

r_c = crop diffusion resistance for water vapour transport ($s.m^{-1}$)

The crop resistance term in this equation is a method of expressing the physiological control mechanisms of a crop by which the crop restricts the rate of evapotranspiration. Diffusion resistance of the crop, r_c, is the reciprocal sum of the cuticular resistance and the stomatal resistance of that crop. Cuticular resistance is at least of an order of magnitude higher than stomatal resistance for a given crop. The diffusion resistance of a crop can therefore be represented approximately by the stomatal resistance r_s (Monteith, 1973).

Soer (1977) has found that a simple resistance model provides satisfactory estimates of the stomatal resistance.

$$r_s = h^{-0.5}\left(1.69\times10^{-1}\angle(-\psi_L)^{XC} + \frac{400}{R_s+1.5}\right) \qquad (22)$$

where

$$-0.7 \text{ MPa} > \psi_L > -5.0 \text{ MPa}$$

ψ_L = leaf water potential (Pa)

h = crop height (m)

r_s = standard resistance ($s.m^{-1}$)

XC = optimisation constant.

The limits on the water potential of leaves were suggested by Rijtema (1965) as the minima and maxima for which r_s varies with ψ_L.

The value for the optimisation constant XC was found to be 2.3 by using an optimisation technique. Rijtema (1965) suggested a value of 2.1 but this gave less satisfactory results in this study.

3.4.1 Leaf Water Potential (ψ_L)

The evapotranspiration flux can be calculated from the water flux through the soil and plant as described by Feddes and Rijtema (1972):

$$E = \frac{1}{g} \frac{\psi_L - \psi_s}{r_{PL} + r_{so}} \qquad (23)$$

ψ_L = leaf water potential (Pa)

ψ_s = soil water potential (Pa)

r_{PL} = plant resistance for water transport (s)

r_{so} = soil hydraulic resistance (s)

where

$$r_{so} = \frac{b}{K(\psi_g)} \qquad (24)$$

b = root density resistance factor (m)

$K(\psi_s)$ = hydraulic conductivity for the soil ($m.s^{-1}$)

and

$$K(\psi_s) = K_s \frac{\psi_s}{\psi_a}^{-(1.4+3m)} \qquad (25)$$

K_s = saturated hydraulic conductivity ($m.s^{-1}$)

ψ_s = soil water potential (Pa)

ψ_a = air entry value of soil (Pa)

m = pore size distribution factor.

The resistance factor due to root density, the saturated hydraulic conductivity, the plant resistance, the air entry value and the pore size distribution factor have little effect on the value of the evapotranspiration flux. It is therefore acceptable to estimate values for these factors from the values for 'standard' soils given by Soer (1977) and Rijtema (1965) (see section 5.1.4).

Now, the energy balance components may be used to calculate E for any one iteration. Thus,

$$E = -\frac{(R_n+G+H)}{L} \qquad (26)$$

L = latent heat of vapourisation ($J.Kg^{-1}$)

Hence by combining equations (23) and (26) it is possible to estimate a value for the leaf water potential and this value may then be used in equation (22) to obtain a value for the stomatal resistance, r_s.

3.5 The Ground Heat Flux

The heat flux in the soil, G, is the most difficult component of the energy balance equation to estimate accurately without a detailed knowledge of the properties of specific soils. This is because the thermal properties of a soil are highly dependent on the moisture content and the degree of compaction of that soil.

Expressions for calculating the thermal properties of a soil by considering the volume fractions, the geometry and the specific conductivities of the components of that soil are available (De Vries, 1975). This approach has been followed by Soer (1977) to calculate G using an explicit finite difference scheme to solve the equation for the transport of heat into the soil. The need for such a detailed knowledge of the soil makes this approach unsuitable for a remote sensing survey.

Other workers in this field have ignored the heat flux in the soil because of its relative unimportance in the energy balance equation. The models of Manabe, et al. (1974) and Gates (1975) do not include an estimate of the ground heat flux. Their approach gives a reasonable agreement during the day, when the heat flux in the soil is usually small compared to the other energy balance components, but large errors sometimes occur during the night when the ground heat flux is often the major component in the energy balance equation.

In an effort to avoid such errors, several workers have related the heat flux in the soil to one of the other components of energy balance. Idso et al. (1975) suggested that the soil heat flux is proportional to the net radiative flux using a proportionality constant of 0.4. Kashera and Washington (1971) and Sasamori (1970) suggested that the heat flux in the soil can

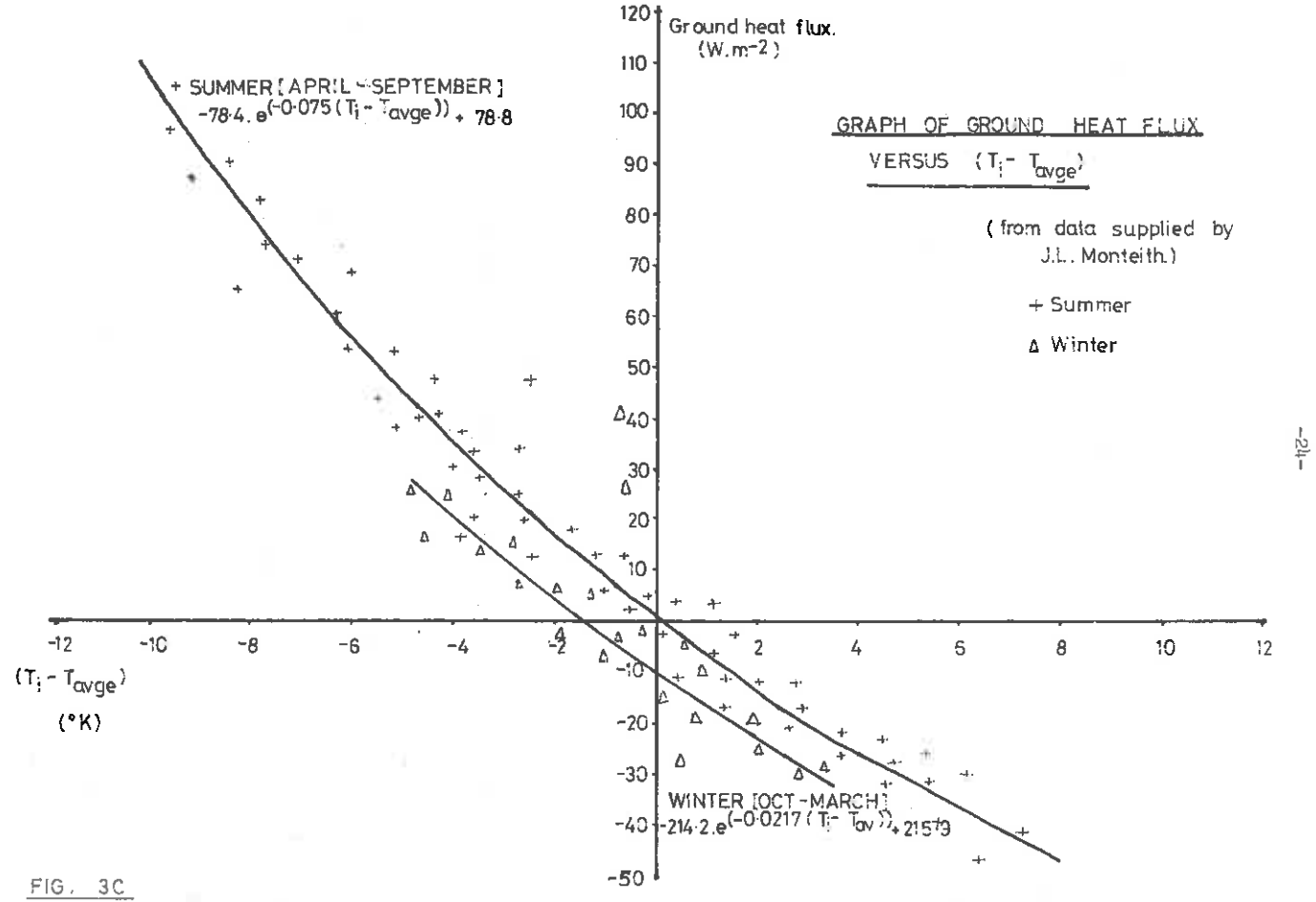
Ground heat flux.
(W.m-2)
+ SUMMER [APRIL - SEPTEMBER]
-78·4. e(-0·075 (Ti - Tavge)) + 78·8
GRAPH OF GROUND HEAT FLUX
VERSUS (Ti - Tavge)
(from data supplied by J.L. Monteith.)
+ Summer
Δ Winter
WINTER [OCT - MARCH]
-214·2.e(-0·0217 (Ti - Tav)) + 215·9
(Ti - Tavge)
(°K)
120
110
100
90
80
70
60
50
40
30
20
10
-10
-20
-30
-40
-50
-12
-10
-8
-6
-4
-2
2
4
5
8
10
12

FIG. 3C

be assumed to be one third of the sensible heat flux. Recent research has shown however that the approximations can produce large errors under specific environmental conditions (Soer, 1977; Rosema, 1975).

A comparison of a number of methods of estimating soil heat flux has been undertaken by Deardorff (1978), who concluded that the multilayer approach used by Soer (1977) and Benoit (1976) was more accurate than any of the other approaches. Since a multilayer approach is inappropriate for a remote sensing survey, an attempt was made to improve upon the empirical approach which have been used so far.

Figure 3c shows a graph of the soil heat flux against the difference between the average diurnal crop temperature and the actual temperature of the crop. A computer optimisation technique was then used to obtain a mathematical expression to describe this relationship. This expression is as follows:

$$G_i = A.e^{B(T_{avge} - T_i)} + C \qquad (27)$$

G_i = ground heat flux ($w.m^{-1}$)

T_i = crop temperature (K)

T_{avge} = average diurnal crop temperature (K)

A,B,C = are constants.

The values for the constants A,B and C were found using a computer optimisation technique. A greater accuracy was obtained when different values for these constants were used for winter and summer. The following constants were used:

SUMMER (April-September)

$$G_i = -78.4.e^{|-0.0755(T_{avge} - T_i)|} + 78.8 \qquad (28)$$

WINTER (October-March)

$$G_i = -214.2 \cdot e^{|-0.0217\ (T_{avge} - T_i)|} + 215.9 \qquad (29)$$

These empirical relationships give good agreement using soil heat flux data obtained from Monteith (pers. comun.).

3.6 Boundary Conditions

Boundary conditions are necessary to solve the transport equations for heat and water flow from the soil into the atmosphere. As the simulation model is dynamic these boundary conditions must also be dynamic, except those which are constant with time.

The boundary conditions for water flow are the water pressures at reference levels in the atmosphere and the soil. Values for water vapour pressure are provided by hourly measurements of wet bulb and dry bulb temperatures in the atmosphere. A value for the water pressure in the soil is estimated from the look-up table version of this model as described in section 4.4. The latter boundary condition is not dynamic as the value of the soil water pressure is assumed to be constant for a diurnal period.

The boundary condition for heat flow in the atmosphere is simply the temperature at some reference level. A boundary condition for heat flow in the soil on the other hand is not required since an empirical approach described in section 3.5 will be used to calculate the soil heat flux.

The final boundary condition is the energy balance equation at the surface of the crop. The model uses an iterative approach to obtain a value for the temperature of a crop from the energy balance equation.

4. Computing Strategy

4.1 Input data

The input data are summarised in table 1. The model was designed so that its requirement for data would be provided by routine measurements taken at local meteorological stations and by remote sensing.

The dynamic inputs of dry bulb temperature, wet-bulb temperature, wind velocity and cloud cover can be provided by routine measurements made at local meteorological stations. There may be a problem in the spatial interpolation of these measurements over nearby crop because of the lack of horizontal homogeneity in most agricultural regions which are economically important. Interpolation errors will be investigated by taking simultaneous measurements of selected parameters above the crop and at local meteorological stations. The intensive ground truth campaigns during the recent aircraft experiments will allow the investigation of interpolation errors.

4.2 Simulation Output

The output from this model is in tabular form as shown in tables 3 and 4. Table 3 reproduces the dynamic meteorological inputs for the model. The second table contains the results of the simulation program.

Table 2 lists the output parameters and their units.

TABLE 1. Input Parameters (Channel 5)

CARD 1:	IYEAR	- Year
	IMONTH	- month
	IDAY	- day of month
	NAMES	- name of month in alphanumeric characters
CARD 2:	ZONG	- Longitude (^{0} east of Greenwich)
	ZAT	- Latitude
	EC	- emission coefficient ($\sim$0.95)
	REFL	- dummy reflection coefficient ($\sim$0.330)
	CH	- high cloud fraction (tenths)
	CM	- medium cloud fraction (tenths)
	CL	- low cloud fraction (tenths)
CARD 3:	MIN	- time of diurnal minimum crop temperature (hours)
	MAX	- time of diurnal maximum crop temperature (hours)
	GMT	- conversion from local time to Greenwich mean time (hours)
CARD 4:	GHC	- Crop height (m)
	ZR	- Reference level in the atmosphere (m)
	PA	- Mean air pressure during diurnal period (Pa)
	TPO (MIN)	- Minimum diurnal crop temperature (^{0}K)
	TPO (MAX)	- Maximum diurnal crop temperature (^{0}K)

CARDS 5-28: (One card for each time step)

TPA(I)	- Dry-bulb air temperature (^{0}C)
TPW(I)	- Wet-bulb air temperature (^{0}C)
U(I)	- wind velocity (m.s^{-1})

CARD 29:	RD	- Root density resistance factor (m)
	PSIA	- Air entry value of soil (kPa)
	BL	- Pore size distribution factor
	AKO	- Saturated hydraulic conductivity (m.s^{-1})
	RPL	- Plant resistance for water transport (s)
	PSIS	- Soil water pressure (Pa)

TABLE 2. Output Parameters

TIME - local time (hours)

RNI - net radiation flux ($w.m^{-2}$)

GHF - ground heat flux ($w.m^{-2}$)

H - sensible heat flux ($w.m^{-2}$)

ALE - latent heat flux ($w.m^{-1}$)

EVAP - hourly evaporation (mm)

DEW - dew accumulation (mm)

CROP TEMP - crop temperature (K)

RA - turbulent diffusion resistance ($s.m^{-1}$)

RC - crop diffusion resistance ($s.m^{-1}$)

PSIL - leaf water pressure (Pa)

AMOL - monin-obukhov length (m)

RESULTS OF SIMULATION ANALYSIS

SIMULATION FOR MAY 26 1970

LONGITUDE 292.10 LATITUDE 50.80

TIME	AIR TEMP.	U-V	VAP. PRES.	CLOUD
1	288.4	1.9	1385.	0.0/0.0/0.0
2	287.5	1.7	1331.	0.0/0.0/0.0
3	286.9	1.8	1296.	0.0/0.0/0.0
4	286.1	1.8	1245.	0.0/0.0/0.0
5	285.0	0.9	1079.	0.0/0.0/1.0
6	282.7	0.9	1036.	0.0/0.0/1.0
7	284.3	0.9	1039.	0.0/0.0/0.0
8	284.9	0.9	1084.	1.0/0.0/0.0
9	289.7	1.8	1228.	0.0/0.0/0.0
10	291.0	2.0	1160.	0.0/0.0/0.0
11	291.9	2.1	1126.	0.0/0.0/0.0
12	293.2	2.7	1170.	0.0/0.0/0.0
13	294.1	3.1	1121.	0.0/0.0/0.0
14	294.1	2.8	1121.	0.0/0.0/0.0
15	293.8	2.3	1019.	0.0/0.0/0.0
16	295.4	2.0	1078.	0.0/0.0/0.0
17	295.6	2.2	1048.	0.0/0.0/0.0
18	295.6	1.5	1028.	0.0/0.0/0.0
19	295.5	1.0	1020.	0.0/0.0/0.0
20	296.3	1.3	1035.	0.0/0.0/0.0
21	291.3	1.3	1284.	0.0/0.0/0.0
22	288.9	1.4	1114.	0.0/0.0/0.0
23	288.4	1.9	1079.	0.0/0.0/0.0
24	288.4	2.9	1078.	0.0/0.0/0.0

TABLE 3 : TYPICAL INPUT TO SIMULATION MODEL

TIME	RNT	GHF	H	ALE	EVAP	PRW	CROP TEMP	RA	RC	PSIL	ABUL
1	-23.5 0.000001	38.0	39.8	-4.3	-.00029	0.00000	286.1	60.8	999.0	0.0	20.0
2	-48.7 0.000001	47.4	21.7	-8.1	-.00045	0.00000	282.9	115.5	999.0	0.0	5.2
3	-61.8 0.000001	51.6	7.9	3.0	0.00033	0.00032	281.8	342.6	0.0	0.0	1.4
4	-63.3 0.000001	51.4	6.9	3.8	0.00352	0.00084	288.2	342.6	0.0	0.0	1.4
5	-62.0 0.000001	51.0	4.7	3.1	0.00450	0.01434	279.3	900.1	0.0	0.0	1.4
6	-65.0 0.000001	55.0	5.7	3.4	0.00494	0.01928	279.3	845.8	0.0	0.0	1.4
7	-39. 0.000104	44.6	2.4	-8.8	-.01280	0.00648	284.1	197.2	0.0	0.0	7.4
8	59.9 0.230104	32.0	7.4	-188.2	-.14092	0.00000	288.2	83.8	0.0	0.0	36.7
9	152.9 0.373311	3.8	-111.7	-44.7	-.00523	0.00000	296.5	36.4	388.4	-1.3	-7.5
10	259.9 0.536401	-24.3	-173.6	-62.4	-.00196	0.00000	298.7	26.5	468.3	-1.4	-9.5
11	357.1 0.700031	-41.3	-242.3	-72.3 ENERGY BALANCE	-.10036 IS NOT ZERO	0.00000	300.7	25.2	525.8	-1.5 **********	-15.2
12	436.2 0.826721	-57.5	-297.2	-80.0	-.11775	0.00000	302.4	21.7	557.3	-1.2	-13.9
13	471.9 0.900421	-66.8	-343.4	-81.4	-.13642	0.00000	305.0	23.2	626.8	-1.0	-10.9
14	476.9 0.911114	-96.6	-385.0	-95.0	-.14316	0.00000	305.7	20.2	648.9	-1.0	-9.0
15	445.9 0.844711	-96.0	-251.6	-94.7	-.13976	0.00000	305.7	24.4	649.2	-1.0	-7.0
16	376.9 0.729431	-92.6	-190.1	-93.2	-.14004	0.00000	305.4	28.3	643.2	-1.0	-7.9
17	285.6 0.613731	-74.4	-122.3	-89.2	-.13180	0.00000	303.9	31.9	611.4	-1.0	-11.6
18	183.0 0.454421	-54.6	-68.9	-79.7	-.11778	0.00000	302.1	38.6	559.7	-1.3	-17.0
19	85.1 0.267701	-29.5	9.4	-66.7	-.09569	0.00000	299.3	66.6	483.2	-1.6	38.9
20	3.6 0.123041	9.1	9.1	-22.3	-.03287	0.00000	293.4	454.1	296.3	-1.1	1.6
21	-51.1 0.000301	12.3	42.2	-4.4	-.00644	0.00000	288.1	321.5	999.0	0.0	1.4
22	-46.6 0.000001	12.9	40.2	-6.6	-.00968	0.00000	288.0	183.8	999.0	0.0	4.3
23	-58.5 0.000001	42.0	17.0	-1.4	-.00210	0.00000	286.7	321.5	999.0	0.0	1.4
24	-57.5 0.000001	42.4	16.0	-1.8	-.00257	0.00000	286.9	368.2	999.0	0.0	1.4

TOTAL EVAP FOR SIMULAT PERIOD = 1.48389

TABLE 4 TYPICAL OUTPUT FROM SIMULATION MODEL

4.3 COMPUTING STRATEGY

4.3.1 The Iteration Procedure

An iterative process is required to balance the energy balance equation at each time step. The time step used in the model is one hour and this period is too great to allow the value of the crop temperature at the previous time step to be used as the initial value for the current time step. For this reason the first approximation for the temperature of the crop of each time step is provided by a temperature curve fitted between the maximum and minimum crop temperature which one measured by an infrared radiometer such as the HCMR on the Applications Explorer Mission - A.

The upper and lower limits on the iteration procedure are the first approximation of the temperature of the crop plus or minus ten degrees. The maxima is called TPR and the minima TPL. If for any particular approximation of the crop temperature the energy balance equation is not equal to zero a new value is calculated according to Bolzano's method:

$$\text{IF (ENBA.GT.0.) TPR = TPO}$$

$$\text{IF (ENBA.LT.0.) TPL = TPO}$$

$$TPO^{n+1} = \tfrac{1}{2}\,(TPL+TPR)$$

where ENBA is the sum of the energy balance components, TPO is the crop temperature and n is the iteration step. The search for the correct value for the temperature of the crop stops when the absolute value of ENBA becomes smaller than 1.0 $W.m.^{-2}$.

4.3.2 Calculation of the first approximation for crop temperature in the iteration procedure

To obtain a first approximation for the crop temperature a curve is fitted between the maximum and minimum crop temperatures

supplied by the remote sensor. To obtain the geometry of the curve a fourier analysis was undertaken for each month of hourly average temperature using data supplied by Monteith (pers. commun.) (figure 4a):

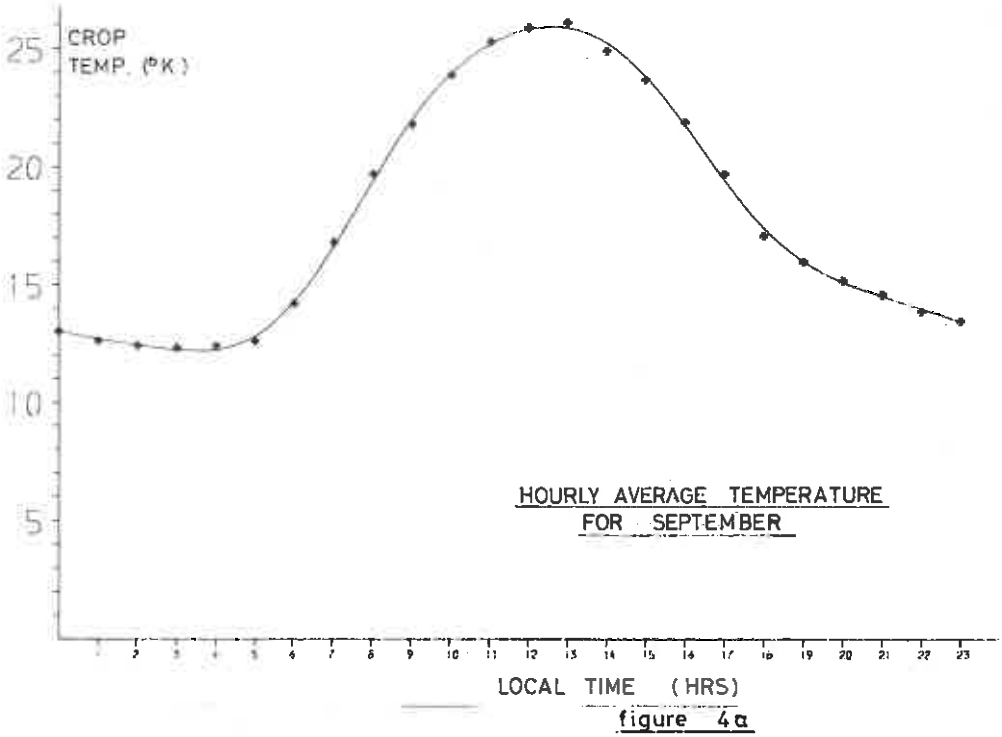

figure 4a

4.4 The "Look-up" Table

The aim of this model is to estimate a value for the soil moisture potential from the meteorological data in section 4.1. It would be possible to use an iterative technique to find a value for soil moisture potential that gives simulation results that correspond closely to the information given by the remote sensor. Such a technique would require a great deal of computer time.

A more economical solution to the problem is to use a "look-up" table as shown in table 5. A range of predetermined values for the two unknown variables, namely the soil moisture potential and the height of a crop are used in the simulation model to produce values for the maximum and minimum crop temperature. These are displayed in tabular form. By inspection of the table, it is possible to determine the likely values for crop height and soil moisture potential. These values can then be used as discrete inputs to the simulation model to obtain a complete simulation output as shown in tables 3 and 4.

**** SOIL TEMPERATURE - EVAPOTRANSPIRATION - DATADOR ON THE 4 AUG 1970 ****

CROP HEIGHT (M)		SOIL WATER PRESSURE (PA)				
		1.0	10.0	100.0	1000.0	10000.0
0.10	DAY.TEMP.:	305.2	306.6	304.9	305.3	309.2
	NIG.TEMP.:	282.1	282.1	282.2	282.1	282.2
	EVAP.:	-1.17	-1.41	-1.23	-1.25	-0.21
0.25	DAY.TEMP.:	302.8	302.8	303.1	305.7	306.9
	NIG.TEMP.:	283.1	282.9	282.9	282.9	282.9
	EVAP.:	-4.93	-4.01	-3.85	-1.43	-0.27
0.50	DAY.TEMP.:	301.5	301.5	301.7	303.9	304.8
	NIG.TEMP.:	283.3	283.3	283.3	283.8	283.8
	EVAP.:	-4.93	-4.57	-4.54	-1.72	-0.35
1.00	DAY.TEMP.:	300.1	300.3	300.3	301.3	302.4
	NIG.TEMP.:	284.5	284.5	284.5	284.5	284.5
	EVAP.:	-5.50	-5.32	-5.04	-1.85	-0.26

TABLE 5.

5. *RESULTS*

One aim of this study was to test this model with data collected in the UK as part of the Tellus project (Elkington *1978*). This aim was not achieved however as poor cloud conditions and a long delay in the processing of the satellite images have prevented any satellite data becoming available. The micrometeorological data collected as part of the Canadian Matador project was however found to be suitable for the testing of the model (Ripley et al *(1973)*).

The Matador project was part of the Canadian contribution to the International Biological Programme and involved a study of the ecosystem of a natural grassland area in South-West Saskatchewan, Canada. As part of this project a large number of micrometeorological measurements were taken automatically at hourly intervals from May to November, *1970*. Details of how these measurements were taken are described fully in the reports of the Matador Project and need not concern us here. (Ripley and Redmann *(1976)*).

For the sake of simplicity only the simulations performed for 26^{th} July and 4^{th} August *1970* are presented here. Tables *(6)* and *(7)* show how the input parameters for these two simulations, and tables *(8)* and *(9)* show the corresponding output parameters. Included in tables *(6)* and *(7)* are the measured values for the ground heat flux, the net radiation flux and the crop temperature. These parameters will permit comparisons to be made between them and the estimated values for these variables provided by the simulation model.

5.1 *Simulation results*

5.1.1 *Simulation for 26^{th} July 1970*

The simulation output for 26^{th} July is shown in table *(8)*. Graphs showing simulated and measured values for the crop temperature, the net radiation flux and the ground heat flux are presented in figures *5(a), 5(b) and 5(c)*.

Figure *5(d)* shows the variation in the temperature of the air and the crop during the simulation period. It shows that unstable conditions occured between *0700 and 1830* hours, with a maximum difference between the two temperatures of $6^{o}K$. Stable conditions occurred during the night.

The variation of the energy balance components during the simulation period is shown in figure *5(e)*. Before noon the latent heat flux exceeded the flux of sensible heat. At noon the latent heat flux reaches a plateau

TABLE 6 : MATADOR PROJECT DATA FOR 26th JULY 1970

Soil moisture content **0.29**

Crop height **0.45m**

Emission coefficient **0.95**

Dummy reflection coefficient **0.33**

Cloud factor 0.0

Mean air pressure **93730 pa**

Longitude 252.1 Latitude 50.8

DATA INPUT				MEASURED VALUES		
Local Time	Dry-Bulb temp.	Wet-bulb temp.	Wind speed	Ground Heat Flux	Net Radiation	Crop Temp.
hrs	°K	°K	$m.s^{-1}$	$W.m^{-2}$	$W.m^{-2}$	°K
1	288.4	287.3	1.9	9.8	-28.0	287.3
2	287.5	286.6	1.7	10.5	-35.0	286.4
3	286.5	285.9	0.4	15.4	-42.0	282.1
4	284.1	283.8	1.0	22.4	-21.0	280.4
5	282.9	282.8	0.9	25.2	-14.0	279.3
6	282.7	282.8	0.9	27.3	- 7.0	279.2
7	284.3	283.9	1.0	23.8	35.0	283.4
8	286.9	285.4	1.0	14.0	105.0	287.0
9	289.0	286.3	0.9	1.4	217.0	290.7
10	291.0	286.9	1.4	-20.3	343.0	293.5
11	291.9	287.1	2.1	-37.1	434.0	295.3
12	293.2	287.8	3.1	-58.1	567.0	298.0
13	294.1	287.9	3.1	-72.1	567.0	299.2
14	294.1	287.3	2.6	-76.3	490.0	298.8
15	295.0	287.7	2.3	-70.7	518.0	300.3
16	295.4	287.8	2.0	-66.5	469.0	300.6
17	295.6	287.9	2.2	-52.5	-	300.4
18	295.6	287.9	1.5	-39.2	-	299.0
19	295.5	287.8	1.2	-25.2	182.0	296.7
20	294.5	287.8	1.5	- 9.1	70.0	294.0
21	291.3	287.6	1.3	0.7	-21.1	289.5
22	288.9	285.7	1.4	9.8	-49.0	286.2
23	288.4	285.7	1.9	15.4	-42.0	286.3
24	288.4	285.3	2.4	16.8	-56.0	286.3

TABLE 7 : [illegible] FOR [illegible]

Soil moisture content 0.11

Crop height 0.55 m

Emission coefficient 0.95

Dummy reflection coefficient 0.[illegible]

Cloud factor 0.0

Mean air pressure 93960[illegible]

Longitude 25[illegible].1 Latitude 50.[illegible]

DATA INPUT				MEASURED VALUES		
Local Time	Dry-Bulb Temp.	Wet-Bulb Temp.	Wind Speed	Ground Heat Flux	Net Radiation	Crop Temp.
hrs	°K	°K	$m.sec^{-1}$	$...^{-2}$	$...^{-2}$	°K
1	287.8	285.0	2.2	9.1	-63.[illegible]	284.7
2	285.1	283.7	1.4	11.9	-56.0	282.7
3	284.7	283.4	0.8	17.5	-49.0	280.1
4	283.5	282.6	0.3	18.9	-45.[illegible]	280.0
5	282.9	282.2	0.5	20.[illegible]	-35.0	279.[illegible]
6	282.4	281.7	0.7	21.7	-25.0	27[illegible].5
7	284.5	283.5	0.7	18.2	0.0	2[illegible].[illegible]
8	288.9	286.1	1.5	4.9	122.0	290.5
9	291.1	287.3	1.[illegible]	-7.[illegible]	220.0	294.1
10	294.3	2[illegible].0	2.3	-10.1	357.0	29[illegible].5
11	295.7	289.1	3.1	-45.5	441.0	300.[illegible]
12	296.6	289.5	3.3	-64.4	467.[illegible]	302.[illegible]
13	298.3	289.7	3.4	-71.4	536.0	305.6
14	299.0	289.8	3.[illegible]	-84.4	542.0	306.9
15	299.6	289.9	3.3	-82.6	497.0	306.[illegible]
16	300.5	289.7	2.2	-74.9	441.0	306.8
17	300.5	289.4	2.2	-64.4	364.0	305.7
18	300.4	289.8	1.9	-45.[illegible]	231.0	303.4
19	299.9	29[illegible].0	1.5	-30.[illegible]	13[illegible].0	299.[illegible]
20	297.1	289.5	1.0	-15.4	0.0	293.5
21	294.5	28[illegible].[illegible]	1.4	-4.[illegible]	-42.[illegible]	29[illegible].3
22	291.7	286.8	1.7	2.[illegible]	-49.0	286.9
23	289.5	286.3	1.4	7.0	-48.[illegible]	2[illegible].0
24	290.0	286.1	1.[illegible]	10.5	-52.0	284.6

TIME	RNT	GMF	H	ALF	EVAP	PRV	CROP TEMP	RA	RC	PSIL	AMOL
1	-48.2	22.7	24.8	-0.8	-.00128	0.00000	287.2	54.9	999.0	0.0	22.5
2	-47.8	26.3	20.8	-0.4	-.00052	0.00000	286.4	65.8	999.0	0.0	17.8
3	-48.2	29.6	14.7	4.1	0.00596	0.00594	285.5	82.3	0.0	0.0	13.3
4	-52.3	37.7	7.8	6.5	0.00934	0.01517	283.1	151.3	0.0	0.0	5.9
5	-56.2	41.1	9.8	4.4	0.00720	0.02436	282.0	183.9	0.0	0.0	5.0
6	-53.7	42.4	5.9	4.1	0.00593	0.03055	281.4	261.0	0.0	0.0	2.9
7	-2.3	33.4	-1.6	-29.1	-.04258	0.00000	284.4	99.3	0.0	0.0	9999.0
8	92.1	14.1	-51.0	-56.9	-.07049	0.00000	289.1	49.4	97.4	-0.7	-2.6
9	207.4	-3.7	-93.9	-103.5	-.15182	0.00000	292.4	40.9	96.0	-0.7	-2.3
10	312.6	-19.1	-118.3	-164.7	-.24122	0.00000	294.6	32.1	85.7	-0.7	-8.6
11	409.8	-38.4	-189.5	-184.7	-.27008	0.00000	296.8	29.1	122.1	-0.8	-7.1
12	498.4	-52.7	-241.3	-196.5	-.28866	0.00000	298.5	26.9	142.0	-0.8	1=10.8
13	735.6	-63.7	-267.3	-208.5	-.30362	0.10000	299.5	22.9	157.1	-0.9	1=14.0
14	737.5	-67.2	-260.6	-212.1	-.31151	0.00000	299.9	25.0	165.4	-0.9	-9.2
15	580.0	-72.6	-241.3	-211.2	-.31055	0.00000	300.4	27.2	179.2	-0.9	-7.8
16	439.1	-65.9	-184.8	-187.1	-.30485	0.00000	299.9	30.5	182.1	-0.9	-7.1
17	348.8	-52.0	-99.7	-197.7	-.29076	0.00000	298.5	32.0	144.4	-0.8	1=13.5
18	261.1	-36.2	-86.7	-178.3	-.26714	0.00000	296.8	48.1	115.3	-0.8	1=15.5
19	132.7	-21.9	4.9	-114.9	-.16499	0.00000	295.0	113.6	96.7	-0.7	14.1
20	39.9	-0.5	18.1	-46.6	-.06525	0.00000	291.8	167.1	99.4	-0.7	3.2
21	-33.5	23.8	14.1	-5.1	-.00730	0.00000	287.0	346.2	701.7	-0.7	3.4
22	-47.4	28.8	12.4	-3.1	-.00469	0.00000	285.9	152.4	999.0	0.0	3.3
23	-51.2	25.6	34.4	-3.1	-.00750	0.00000	286.6	60.1	999.0	0.0	13.8
24	-54.7	25.0	34.5	-3.3	-.00776	0.00000	286.7	55.0	999.0	0.0	16.6

TOTAL EVAP FOR DIURNAL PERIOD = -3.10MM

TABLE 8 : SIMULATION RESULTS FOR 26TH JULY 1970

[MATADOR DATA]

TIME	RNI	SHF	W	ALE	EVAP	RAIN	CROP TEMP	RA	RC	PRIS.	ANUL
1	-73.5 0.000001	38.9	39.8	-4.5	-.00037 0.000000	0.000000	290.1	44.0	999.0	0.0	20.8
2	-68.7 0.000004	47.4	21.7	-8.1	-.00043 0.000000	0.000000	287.9	115.5	999.0	0.0	3.2
3	-61.6 0.000001	51.6	7.9	3.0	0.00033 0.000000	0.000000	284.9	362.6	0.0	0.0	1.4
4	-58.3 0.000001	53.4	6.9	3.0	0.00352 0.000000	0.000000	288.2	362.6	0.0	0.0	1.4
5	-62.0 0.000001	55.0	6.7	3.1	0.00430 0.000000	0.01434 0.000000	279.3	999.1	0.0	0.0	1.4
6	-65.0 0.000001	55.0	5.9	3.4	0.00494 0.000000	0.01928 0.000000	279.3	663.8	0.0	0.0	1.4
7	-30.0 0.000001	44.6	2.4	-8.8	-.01240 0.000000	0.000000	284.1	197.2	0.0	0.0	7.4
8	59.0 0.000001	32.0	7.4	-100.0	-.14434 0.000000	0.000000	288.2	83.6	0.0	0.0	36.7
9	158.9 0.000001	3.8	-111.7	-46.7	-.00833 0.000000	0.000000	294.3	36.4	288.6	-1.3	-7.1
10	299.9 0.000001	-24.3	-173.4	-62.6	-.09196 0.000000	0.000000	298.7	28.3	668.3	-1.4	-9.3
11	259.1 0.000001	-41.3	-242.3	-72.2 ENERGY BALANCE IS NOT ZERO	-.10634 0.000000	0.000000	300.7	23.2	525.0	-1.5 **********	-15.2 **********
12	436.2 0.000001	-57.5	-297.2	-80.6	-.11775 0.000000	0.000000	302.4	21.7	557.3	-1.3	-15.0
13	471.9 0.000001	-66.8	-343.4	-81.4	-.13404 0.000000	0.000000	305.0	23.2	626.0	-1.0	-8.9
14	476.9 0.000001	-76.6	-385.8	-85.0	-.14310 0.000000	0.000000	305.7	26.2	668.9	-1.0	-9.0
15	465.9 0.000001	-86.0	-424.6	-86.7	-.13976 0.000000	0.000000	305.7	28.4	649.2	-1.0	-7.9
16	376.9 0.000001	-92.6	-440.1	-85.2	-.14000 0.000000	0.000000	305.6	28.3	663.2	-1.0	-7.9
17	285.4 0.000001	-76.4	-422.3	-89.2	-.13160 0.000000	0.000000	303.9	31.0	611.6	-1.0	-11.4
18	183.0 0.000001	-56.6	-48.9	-79.7	-.11770 0.000000	0.000000	302.1	38.6	539.7	-1.3	-17.0
19	85.1 0.000001	-39.5	9.2	-64.7	-.09569 0.000000	0.000000	299.3	66.8	483.2	-1.4	38.9
20	3.6 0.000001	9.1	9.1	-22.3	-.03287 0.000000	0.000000	293.4	456.1	296.5	-1.1	1.4
21	-35.1 0.000001	32.3	22.2	-4.4	-.00644 0.000000	0.000000	288.1	321.5	999.0	0.0	1.4
22	-46.0 0.000001	32.9	40.2	-6.6	-.00948 0.000000	0.000000	288.0	193.8	999.0	0.0	4.3
23	-58.5 0.000001	42.9	17.0	-1.6	-.00234 0.000000	0.000000	286.7	321.3	999.0	0.0	1.4
24	-57.3 0.000001	42.4	14.8	-1.0	-.00207 0.000000	0.000000	286.9	348.2	999.0	0.0	1.4

TOTAL EVAP FOR DIURNAL PERIOD = -1.48300

TABLE 9 : SIMULATION RESULTS FOR 4TH AUGUST 1970
(MATADOR DATA)

SIMULATION FOR 25/7/70 : COMPARISON OF SIMULATED [SOLID] AND MEASURED [BROKEN] VALUES.

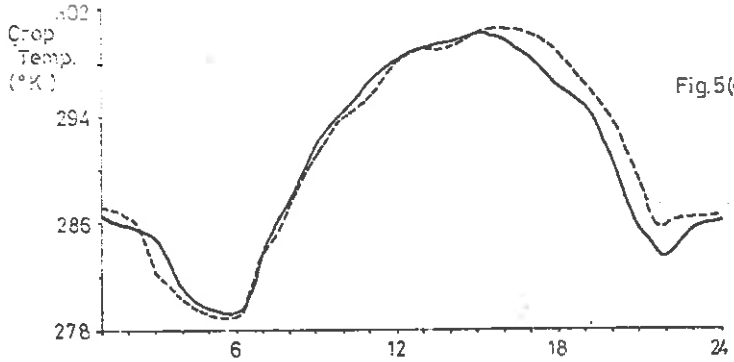

Fig. 5(a): Crop Temperature.

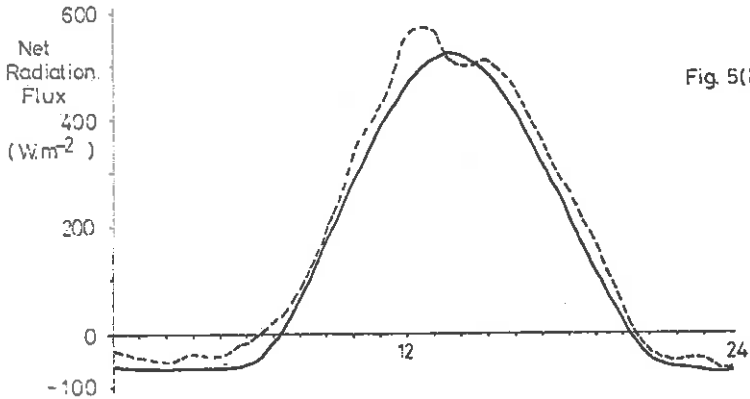

Fig. 5(b): Net Radiation Flux.

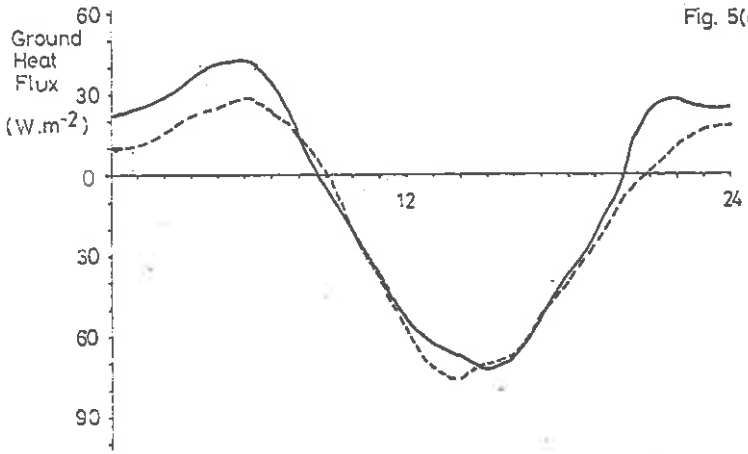

Fig. 5(c): Ground Heat Flux.

SIMULATION FOR 26/7/70 :

Fig. 5(d): Air and crop temperature vss time.

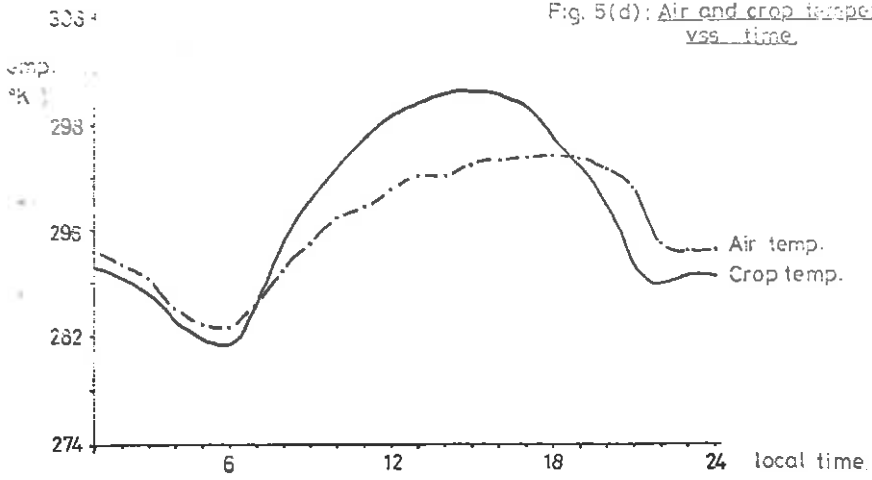

Fig. 5(e): Energy balance components vss time.

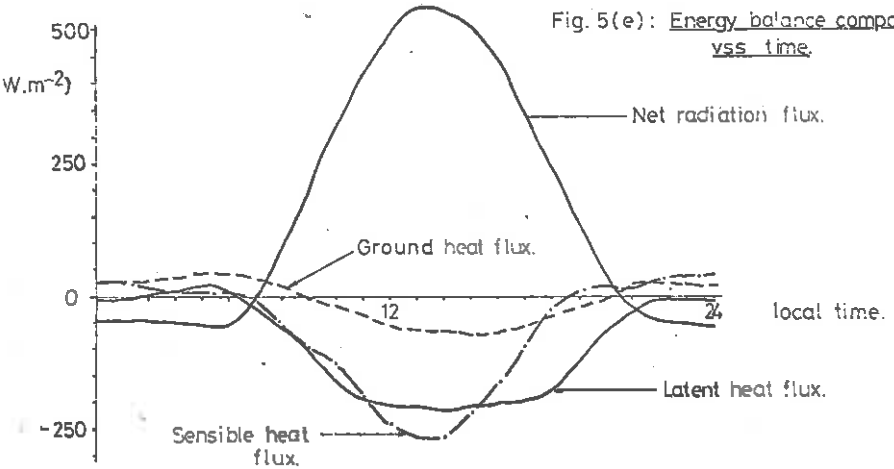

of -200 w.m^{-2} and the sensible heat flux continues to increase to balance the increasing net radiation flux. As the net radiation flux begins to decrease rapidly at 1500 hours the sensible heat flux also falls quickly. The latent heat flux continues at approximately -200 w.m^{-2} until 1800 hours.

Dew appears at 0300 hours when the evaporative flux becomes positive. The crop resistance (r_c) is set at zero when dew is forming. The dew has evaporated by 0700 hours.

The total evaporation for the diurnal period is -3.1 mm. Measurements of the soil water content before and after the simulation period a loss of moisture of -2.5 mm. The difference between the simulated and measured water loss (assuming no run-off) is within the bounds of the experimental errors involved in traditional methods of determining the soil moisture contents.

In figure 5(a) there is a good agreement between the simulated and measured crop temperatures until 1600 hours. After this the measured crop temperature is up to $2^{o}K$ greater than the simulated values. The simulated values for the net radiation flux also show good agreement with the measured values except for the period around noon where the simulated values are approximately 10% lower than the measured values. A secondary peak of 1500 hours is evident in the measured values of net radiation. Figure 5(c) shows a large deviation during the night between the measured and simulated values of the ground heat flux.

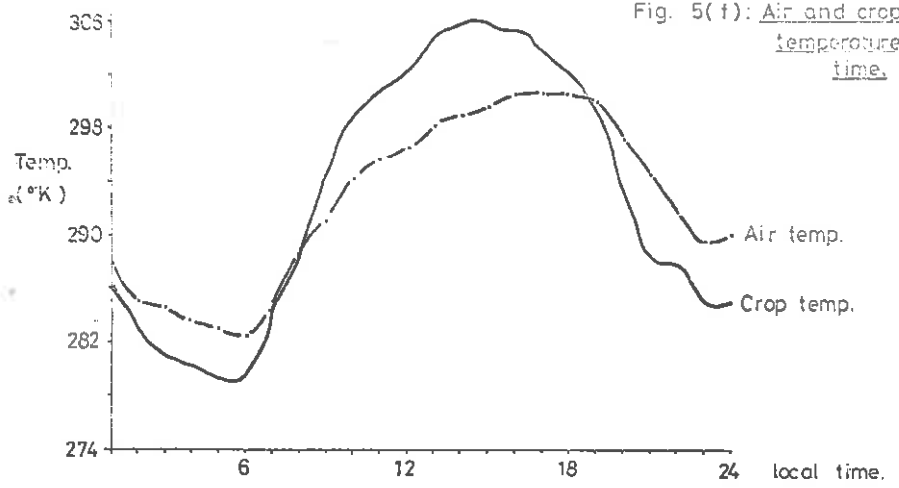

Fig. 5(f): Air and crop temperature vss time.

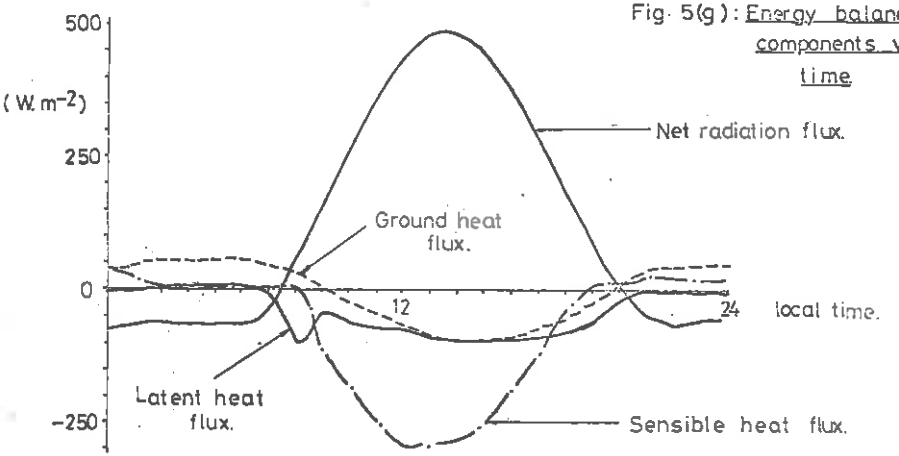

Fig. 5(g): Energy balance components vss time.

SIMULATION FOR 4/8/70 :

SIMULATION FOR 4/8/70 : COMPARISON OF SIMULATED [SOLID] AND MEASURED [BROKEN] VALUES.

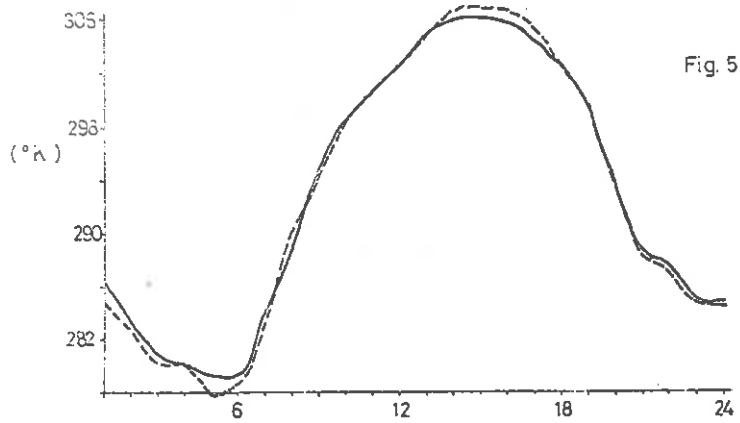

Fig. 5 (h) : Crop temperature

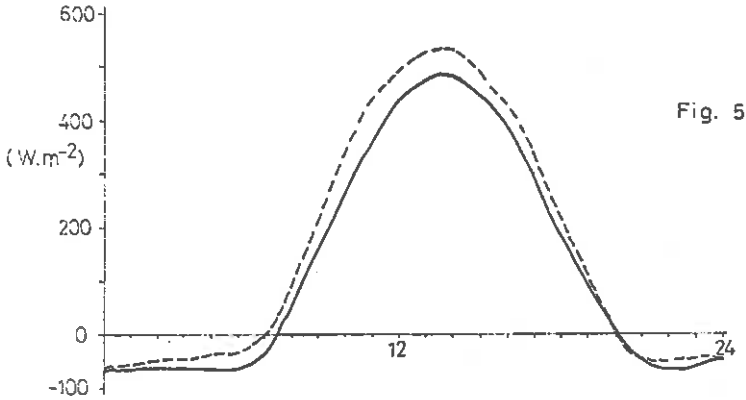

Fig. 5(i): Net radiation flux.

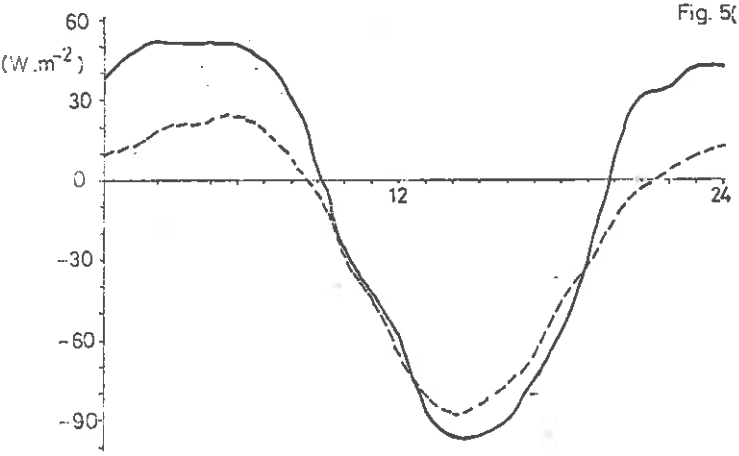

Fig. 5(j): Ground heat flux.

5.1.2 Simulation for 4th August 1970

The results of this simulation differ from those of 26th July as in this case the soil is considerably drier. The simulation results for 4th August are shown in Table (9).

The variables in temperature of the air and crop during the simulation period shown in figure 5(f). There is a period of high instability during the day with the temperature of the crop $8^{o}K$ above the ambient temperature of the air at 1300 hours.

Variations in components of the energy balance equation are shown in figure 5(g). The evaporative flux is reduced for this simulation period and to counter this the sensible heat flux has increased to a maxima of $-3\ w.m^{-2}$ at 1300 hours. Dew occurs, when the evaporative flux is positive, between 0300 and 0700 hours.

The results of the simulation give the total evaporation from the soil and crop over the 24 hour period as -1.48 mm. This is close to the moisture loss given by soil moisture measurements taken before and after the simulation period which produced a moisture loss of -1.9 mm.

Figure 5(h) shows the good agreement between the simulated and measured crop temperatures throughout the simulation period. The simulated value for the crop temperature exceeds the measured value during the night by approximately $0.8^{o}K$. A small error also occurs in the afternoon.

A systematic deviation between the measured and simulated values of the net radiation flux during the day is shown in figure 5(j). The comparison of measured and simulated values of the ground heat flux (figure 5(j)) shows a large deviation during the night.

5.1.3 The effect of soil moisture on the simulation results

To assess the relative importance of soil moisture content on the results of the simulation the model was run for three different values of soil moisture potential using data of 4th August 1970. The values of soil moisture pressure used were -1.0 Pa ('wet'), -1000.0 Pa ('actual') and -1,000,000.0 Pa ('dry'). The results of these simulations are shown in figures 5(k) to 5(o).

As expected there is marked difference between the course of the

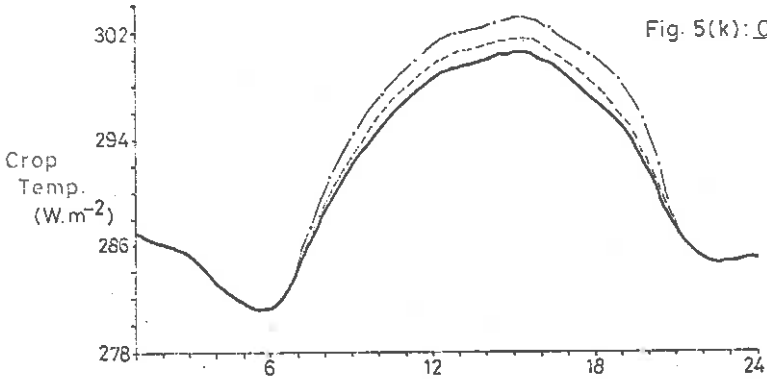

Fig. 5(k): Crop temperature

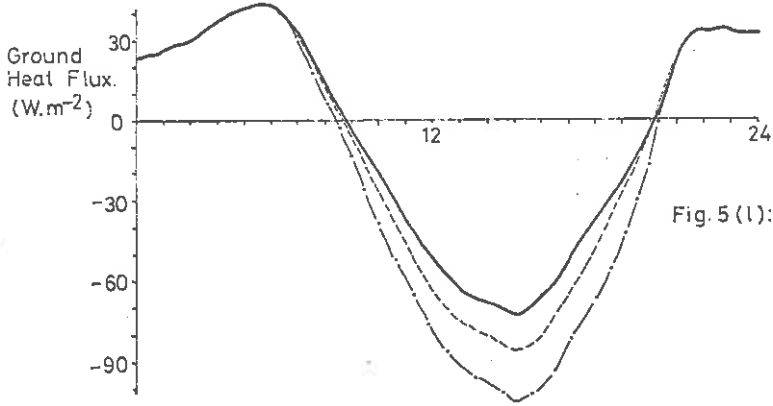

Fig. 5 (l): Ground heat flux.

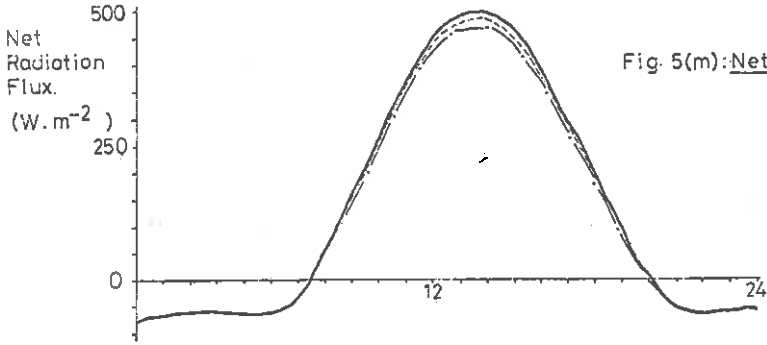

Fig. 5(m): Net radiation flux.

SIMULATION FOR 26/7/70: COMPARISON OF SIMULATION RESULTS FOR VARYING SOIL MOISTURE CONTENT.

KEY: —·— 'dry' ----- 'actual' ——— 'wet'

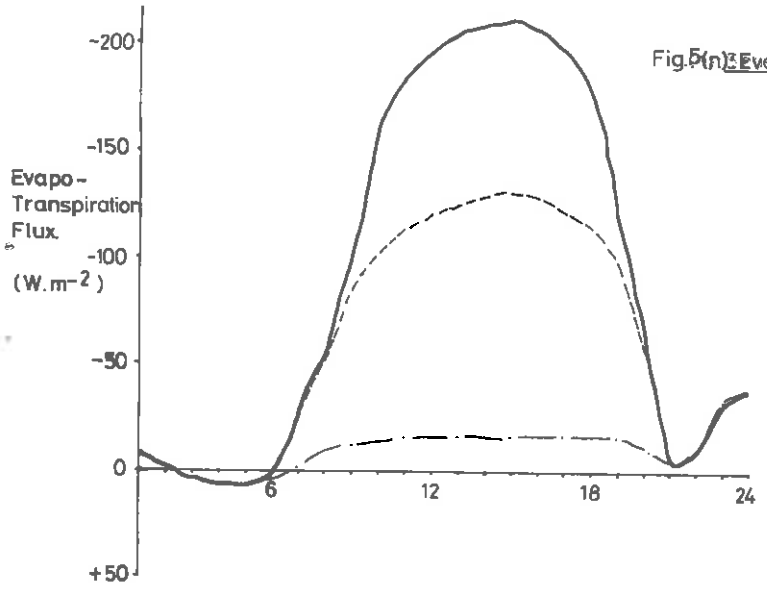

Fig.5(n): Evapotranspiration Flux.

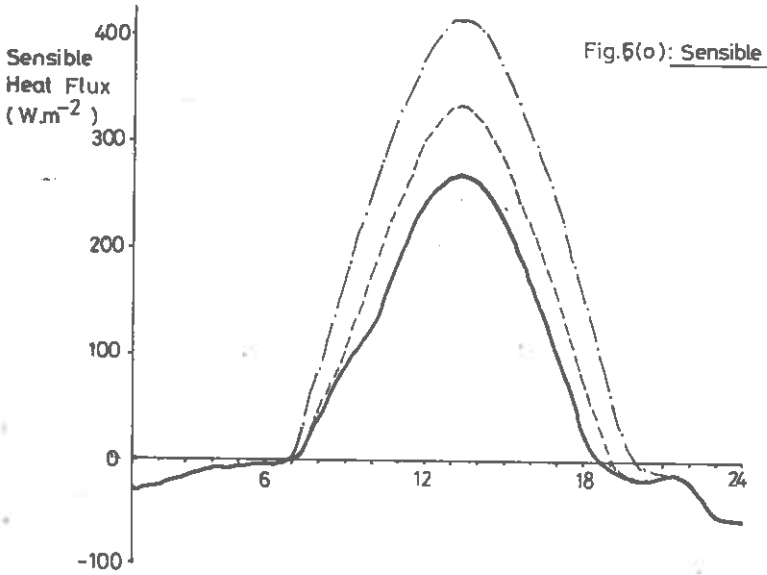

Fig.5(o): Sensible Heat Flux.

SIMULATION FOR 26/7/70 : COMPARISON OF SIMULATION RESULTS FOR VARYING SOIL MOISTURE CONTENT.

KEY: —·— 'dry' - - - - - 'actual' ——— 'wet'

evaporative flux for 'wet' and 'dry' soils (Figure *5(m)*). The total evaporation for the 'wet' soil simulation is *4.03 m* which is considerably less than the *0.27 mm*, evaporation for the simulation of the 'dry' soil.

The diurnal course of the ground heat flux and the sensible heat flux is affected by variations in the soil moisture potential. The 'dry' simulation produces the greatest value during the day for these two energy balance components.

The variation of the soil moisture potential affects the crop temperature during the day as shown in figure *5(k)* where the dry simulation results in an increased crop temperature.

5.1.4 *The effect of soil type on the simulation results*

To assess the effect of various soil types on the results of the simulation the soil parameters of a typical fine sand, loamy clay and river deposit were used in three separate runs of the simulation model. The soil properties used in this test were those described by Soer *(1977)*. Table *(10)* lists the properties for each of the three soil types and graphs of the simulation results for temperature of the crop and ground heat flux are presented in figures *5(p)* and *5(q)* respectively.

5.1.5 *The effect of height of the crop on the simulation results*

To determine the effect of different crop heights on the results of the simulation are presented graphically in figures *5(s)*to *5(v)*.

Figure *5(s)* shows that a shorter crop leads to an increased amplitude for the diurnal course of the crop temperature.

5.1.6 *The effect of the emission coefficient on the simulation results*

In all of the proceeding simulations an emission coefficient of *0.95* has been used. This value was chosen because most other workers in this field have used this value owing to a lack of information about the value of the emission coefficient. Recent research by workers at the Institute of Hydrology however has suggested that a coefficient of *0.97* may be more accurate for a crop greater than *0.50 m* in height (Blyth *(pers comm.)*). Soer *(1977)* suggested that a deviation of *0.01* in the emission coefficient would produce a change in the crop temperature of

TABLE 10 : SOIL PROPERTIES .

(after Cole (1977))

SOIL TYPE	b (-)	r_{pl} (h/s)	K_s (m /day.)	Ψ_a (kPa)	m -
FINE SAND	3.0	10000	2.0	-2.5	0.30
CLAY LOAM	3.7	12300	0.01	-2.0	0.42
RIVER DEPOSIT	2.4	8000	0.2	-3.0	0.32

SYMBOLS USED:

- b - root density distribution factor (-)
- r_{pl} - plant resistance for water transport (s)
- K_s - saturated hydraulic conductivity ($m.s^{-1}$)
- Ψ_a - air entry value of soil (Pa)
- m - pore size distribution factor

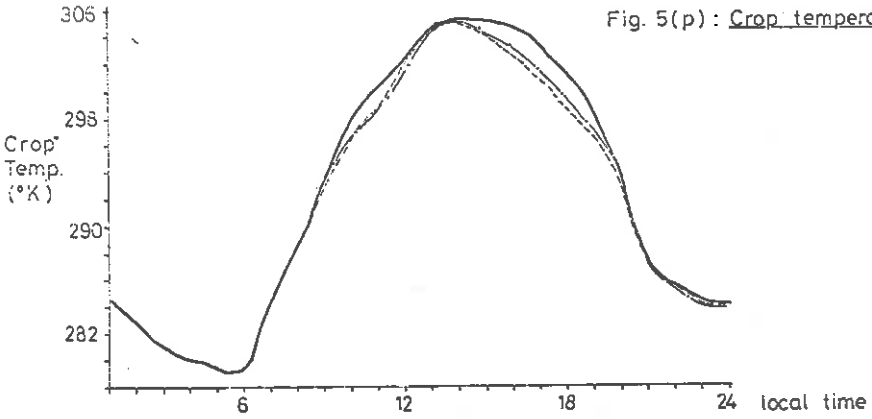

Fig. 5(p) : Crop temperature

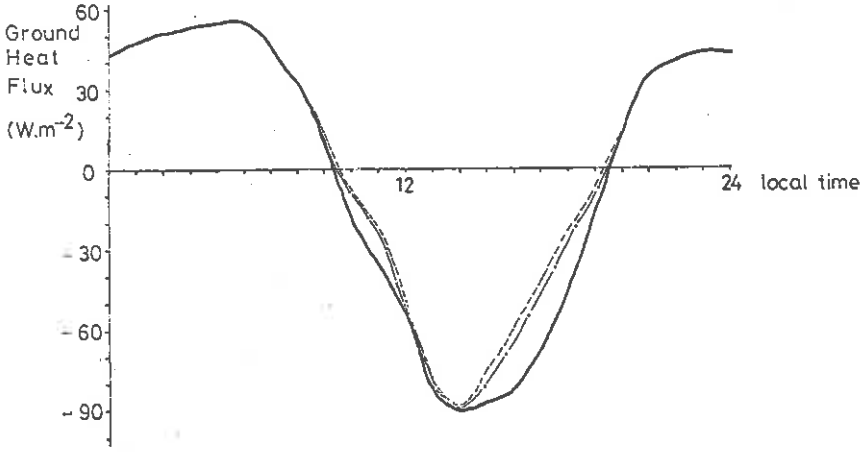

Fig. 5(q) : Ground heat flux.

SIMULATION FOR 4/8/70: COMPARISON OF SIMULATION RESULTS FOR DIFFERENT SOIL TYPES.

KEY:

- River deposit
- Fine sand
- Clay loam

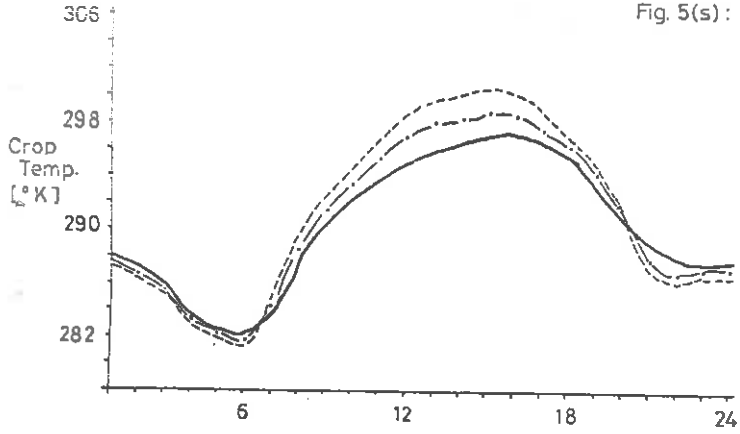

Fig. 5(s) : Crop temperature.

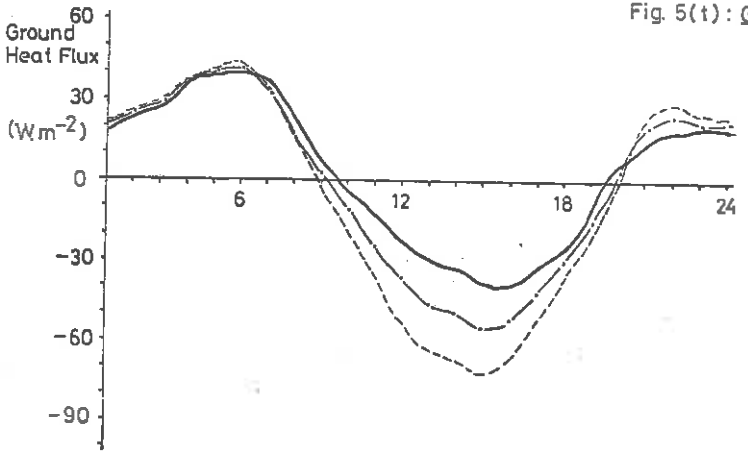

Fig. 5(t) : Ground heat flux.

SIMULATION FOR 26/7/70 : COMPARISON OF SIMULATION RESULTS FOR THREE DIFFERENT CROP HEIGHTS

KEY :

Crop height 0·25 m.
0·50 m.
1·00 m.

Fig. 5(u): Latent heat flux.

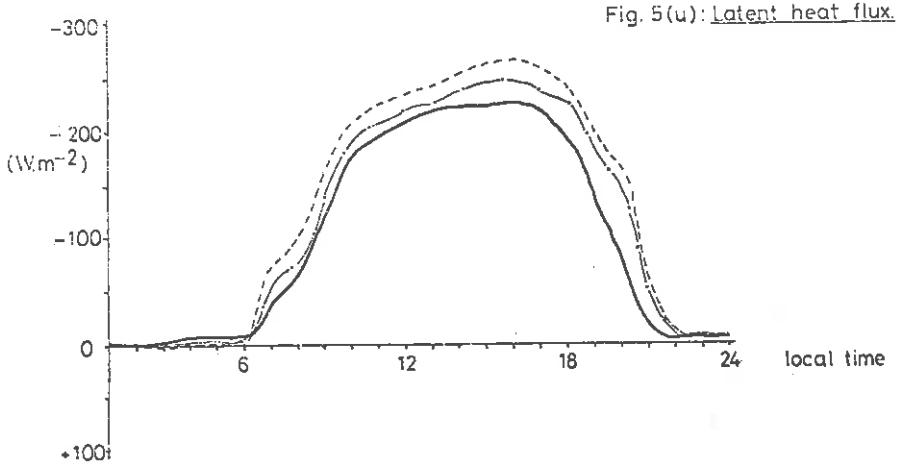

Fig 5(v): Sensible heat flux.

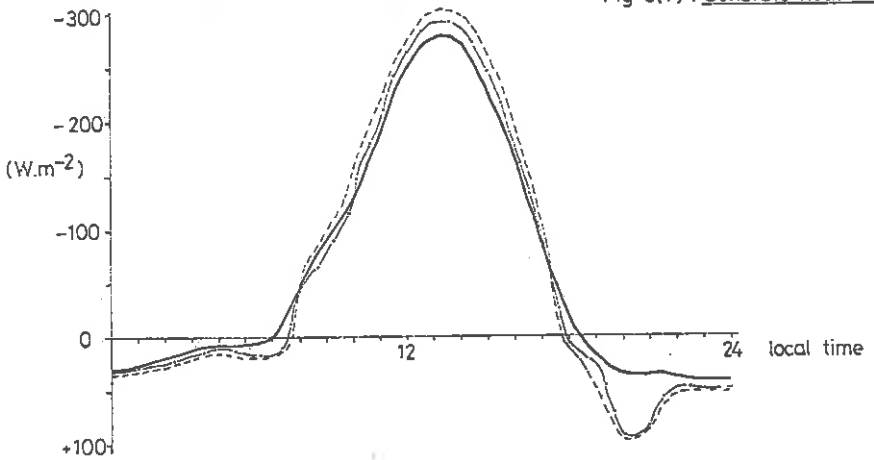

SIMULATION FOR 26/7/70 : COMPARISON OF SIMULATION RESULTS FOR THREE DIFFERENT CROP HEIGHTS.

KEY

Crop height 0·25 m

〃 0·50 m

〃 1·00 m

Fig. 5(w) : The effect of variation of the emission coefficient on the diurnal course of crop temperature.

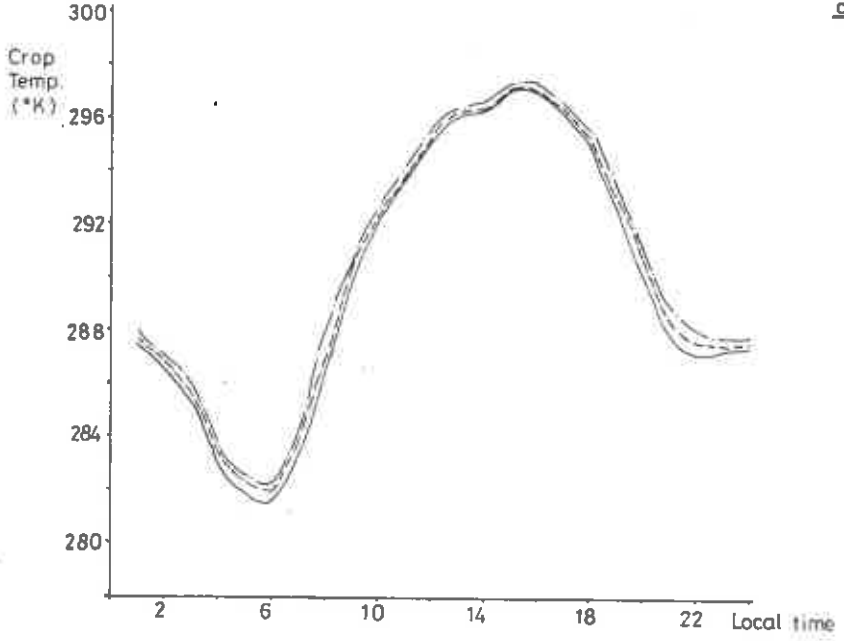

$0.8^{O}K$ when using the TERGRA model. To assess the sensitivity of this model to variations in the emission coefficient three values were used with the input data for 26^{th} July *1970*. Figure *5(w)* shows the simulated crop temperatures for values of the emission coefficient of *0.90*, *0.95* and *1.00*.

The greatest difference between the simulations occurs at dawn and dusk where a larger emission coefficient results in a lower crop temperature.

6. *DISCUSSION*

A number of points for discussion arise from the results presented in Chapter 5. The simulation results for the 26^{th} July and 4^{th} August differ mainly because of the lower moisture content of the soil for the latter simulation. The lower moisture content of 4^{th} August restricts the latent heat flux by stomatal closure (Monteith *(1973)*). Since the latent heat flux cannot then increase to satisfy the energy balance equation the temperature of the crop must rise to allow the sensible heat flux to balance the energy equation.

In both simulations there is a large error between the measured and simulated values for the ground heat flux during the night (figures *5(c)* and *5(j)*). The ground heat flux is a difficult parameter to measure accurately. Indeed many workers place little faith in measurement of this parameter with flux plates as used in the Matador project (Goudriaan *(1977)*). For this reason the algorithm for calculating the ground heat flux will not be altered until further tests on other data sets have been completed.

Although there is a generally good agreement between the measured and simulated values of the crop temperature, two errors appear in each simulation.

The first error occurs around dawn when the simulated crop temperature exceeds the measured value for the crop temperature. An explanation for this could be that the heat storage of the crop, which is ignored in this model, becomes important at this time of the day (Moore et al *(1975)*).

The second error occurs in the afternoon when the simulated crop temperature is less than the measured crop temperature. The crop temperature measurements for the Matador project were made using thermisters attached directly to a leaf rather than by infra-red methods. The contact method is susceptible to errors if direct solar radiation is allowed to influence the thermister readings. Another explanation for this

error stems from a lack of information about the cloud cover conditions during the two simulation periods. The Matador data did not include any cloud cover information and therefore clear sky conditions were assumed. This appears to be a reasonable assumption as indicated by the close agreement between the measured and simulated values of the net radiation flux in both simulations (figs *5(b)* and *5(t)*. The irregularity of the measured values of the net radiation flux on the 26^{th} July however, indicate the presence of clouds during the afternoon. The presence of clouds will have the effect of decreasing the temperature of the crop. The regular course of the measured values of the net radiation flux for the 4^{th} August (fig *5(t)*) is indicative of clear sky conditions and in this case the simulated values for the temperature of the crop agree more closely with the measured values than for the 26^{th} July simulation.

One marked difference between the 'wet' and 'dry' simulation results is the higher crop temperature on the dry soil during the day. The crop on the drier soil does not lose water as quickly as that on the wet soil due to the stomatal control of evaporation. The stomatal control is reflected in the higher values for the crop resistance for the 'dry' soil simulation. The crop resistance on the 'dry' soil reaches an upper limit of *8600* $s.m^{1}$ when the upper limit on the leaf water potential, suggested by Rijtema (1965) as *-5.0 mPa*, is also reached.

There is a maximum difference in the net radiation flux of 30 $W.m^{-2}$ between the simulations for the 'wet' and the 'dry' soil. The higher crop temperature of the 'dry' soil increases the outgoing longwave radiation and therefore decreases the net radiation flux toward the crop.

The effect of different soil types, as shown in figures *5(p)* and *5(q)*, is relatively small compared to the effect of soil moisture on the results of the simulation. The fine sand and river deposits gave similar crop temperatures and similar outputs in other respects. The simulation results for the clay soil differ from the results for the other two soil types primarily because the saturated hydraulic conductivity of the clay is an order of magnitude lower than the other two soil types. The low value for the hydraulic conductivity restricts the transport of the water through the soil which reduces the evapotranspiration flux and therefore has the effect of increasing the crop temperature.

The effect of different crop heights on the temperature of the crop is very marked (figure *5(s)*). An increase in the height of the crop results in a decrease in the amplitude of the diurnal wave of the crop temperature.

This phenomena can be explained by the lower values of the turbulent diffusion resistence (r_a) and the crop diffusion resistance (r_c) which occur with an increase in the height of the crop. The lower values for r_a are due to an increase in the roughness lengths for momentum and sensible heat (Z_{oh} and Z_{om}) which are both directly related to the crop height. The lower values for r_c are due to an increase in the number of stomata with an increase in the height of the crop. The lower crop height results in an increase in the latent heat flux and the sensible heat flux during the day and a decrease in these fluxes during the night.

The effect of variation in the emission coefficient on the results of the simulation as shown in fig. 5(w) is extremely small. During the day a change in the value for the emission coefficient of 0.01 gives a change of $0.1^{o}K$ for the crop temperature. A lower value for the emission coefficient causes a decrease in the emitted longwave radiation which reduces the net radiation flux. A larger deviation between the crop temperatures for different values of the emission coefficient is apparent at night because the emitted longwave radiation is an important component of the energy balance equation during this part of the day.

7. *CONCLUSION*

The results that were obtained using data from the Matador project demonstrate that this model is capable of simulating the diurnal course of the crop temperature and the components of the energy balance equation with data mainly obtained from routine meteorological measurements. Furthermore, the model when used in conjunction with surface temperature measurements, is capable of producing a value for the soil moisture potential and hence the soil moisture content.

The simulation model requires data which cannot be supplied by remote sensing or by routine meteorological measurements. For example the model requires data on the properties of a soil, the emission coefficient of a crop, the soil moisture potential and the height of the crop. It would appear therefore that some field inspection and sampling will always be necessary. There are however several hopeful signs in the results that have been obtained so far which suggest that field inspection and sampling may not always be required or at any rate may be confined to an extent which is economical in practice.

The variation of soil type appears to have little effect on the results of the model. Describing a particular soil in terms of a 'clay' or a 'sand' (as in fig *5(p)* and *5(q)*) appears to produce results which have an acceptable precision in the context of a remote sensing survey.

A change in the value of the emission coefficient appears to have little effect on the simulation results except for the hours around dawn and dusk. There has been insufficient research to date to quantify variations in the emission coefficient of short crops. Preliminary results from the Tellus project have given a value for the emission coefficient over cereal crops of *0.97*. Since most workers in this field have assumed a value of *0.95* for the emission coefficient of a grass canopy, this value will be used until experimental evidence for another value is available.

In contrast to the soil properties and the emission coefficient, the soil moisture pressure and the height of the crop have a marked effect on the results of the simulation model. It is possible to estimate the height of a crop from measurements made on aerial photographs (Thompson, *(1969)*). The main problem is that these photos must be recent to be of value. Another method is to estimate the height of a crop by remote sensing in an infra-red waveband. None of these possibilities are practical at present so values for the crop height must still be supplied by ground inspection.

The model was designed in part to evaluate the soil moisture pressure in the root zone. It would be possible to use an iterative technique to find a value for the soil moisture that gives simulation results which correspond closely to the information given by the remote sensor. This technique would scarcely be economical and would require considerable amounts of computer time. To overcome this problem a "look-up" table will be used as shown in table *(5)*. The "look-up" table produces values for the maximum and minimum diurnal crop temperatures using the simulation model with a number of predetermined values for the soil moisture pressure. Interpolation between the values produced in this table gives an economical method of obtaining a value for the soil moisture pressure. It is then possible to use this value for the soil moisture pressure in the simulation model to produce the complete simulation output, as shown in tables *(8)* and *(9)*.

An objective of this research is to use this model in a remote sensing system to investigate the spatial variation of soil moisture. The

data from the Tellus project will include thermal imagery from the HCMM satellite and the two aircraft experiments that took place during the Summer of *1979*. The thermal imagery will provide surface temperatures which will be used in conjunction with the "look-up" table version of this model to obtain detailed estimates of the soil moisture content over extensive areas.

BIBLIOGRAPHY

Ahmad, S. (1978) The albedo of agricultural and urban surfaces in the Leeds area. Working Paper 217, School of Geography, University of Leeds.

Allen, W.H. (1972) Remote sensing of fallow soil moisture using visible and infrared sensors. University of Texas, Ph.D thesis.

Benoit, R., (1976) A comprehensive parameterisation of the atmospheric boundary layer for general circulation models. MacGill University, Dept. of Meteorology, Ph.D. thesis.

Blanchard, M.B., Greeley, R., and Goettleman, R. (1974) Use of visible near-infrared and thermal infrared remote sensing to study soil moisture. *Proceedings of the 9th Int. Symposium on Remote Sensing Environment.*

Boissard, P., Valery, P., Belluomo, P., and Goillot, C.H. (1978) Assessing the influence of tree hedges on the heat budget at soil level by means of airborne thermography - preview of HCMM capabilities threat. Tellus Report 4, JRC-ISPRA.

Brunt, D. (1939) *Physical and dynamical meteorology.* Cambridge University Press.

Businger, J.A. (1966) Transfer of momentum and heat in the planetary boundary layer. *Proceedings Symp. Arct. Heat Budg. and Atm. Circ.* The Rand Corporation, Santa Monica, 305-22.

Businger, J.A., Wyngaard, J.C., Izumi, Y., and Bradley, E.F. (1971) Flux profile measurements in the atmospheric surface layer. *J. Atm. Sci., 28,* 181-89.

Dawdy, D.R. (1969) Considerations involved in evaluating mathematical modelling of urban hydrologic systems. U.S. Geol. Survey, Water Supply Paper 1591-D.

De Vries, D.A. (1975) *Heat transfer in soils in 'heat and mass transfer in the biosphere'.* In Vries, D.A. and Afgan, N.H. (Eds.) Scripta Book Co., Washington.

Deardorff, J.W. (1978) Efficient prediction of ground surface temperature and soil moisture with inclusion of a layer of vegetation. *J. of Geophys. Res, 83,* No. C4.

Dyer, A.J. (1967) The turbulent transfer of heat and water in an unstable atmosphere. *Quart. J. Roy. Meteorol. Soc., 93,* 501-8.

Edgerton, A.T. (1972) A passive microwave imaging system for soil moisture mapping. Tech. Not TN-366, Aeroject General Corporation, El Monte, California.

Elkington, M.D. (1978) Measurement of soil moisture by remote sensing. Unpublished Report, University of Leeds, School of Geography.

Elkington, M.D. (1979) An approach to characterising the water content of soils by thermal infrared remote sensing. Unpublished Report, University of Leeds, School of Geography.

Feddes, R.A., and Rijtema, P.E. (1972) Water withdrawal by plant roots. *Inst. for Land and Water Management Res. Techn. Bull. No. 83.* Wageningen, The Netherlands.

Fleming, M.D., Berkebile, J.S., and Hoffer, R.M. (1975) Computer aided analysis of landsat 1 MSS data: a comparison of three approaches, including a 'modified clustering approach'. Lars, Purdue Univ., West Lafayette, Indiana, Lars Info, Note 072475.

Fu, K.S., Landgrbe, D.A. Phillips, T.L. (1969) Information processing of remotely sensed agricultural data. *Proc. of the IEEE*, 57(4), 639-53.

Gadd, A.J., Keers, J.F. (1970) Surface exchanges of sensible and latent heat in a 10-level model atmosphere. *Quart. J. Roy. Meteorol. Soc., 96*, 297-308.

Gates, W.L. (1975) The January global climate simulated by a two level general circulation model - a comparison with observations. *J. Atmos. Sci., 32*, 449-77.

Goudriaan, J., and Waggoner, P.E. (1972) Simulating both aerial micro-climate and soil temperature from observations above the foliar canopy. *Neth. J. Agric. Sci, 20*, 104-24.

Hartigan, J.A. (1975) *Clustering algorithms.* Wiley and Sons, New York.

Hoffer, R.M. (1975) Computer-aided analysis of skylab multi-spectral scanner data in mountainous terrain for land-use forestry, water resources and geologic applications. Lars Information Note 121275, Purdue Univ., West Laffayete, Indiana.

Holter, M.R. Courtney, H.W. and Limperis, T. (1970) Research needs - the influence of discrimination, data processing and system design. In Shay, J.R. (Ed.) *Remote sensing with special reference to agriculture and forestry.* Nat. Acad. of Sci., Washington, D.C.

Huff, I.A. (1966) The effect of natural rainfall variability in verification of rain modification experiments. *Water Resources Res, 2*, 791-801.

Idso, S.B., and Ehrler, W.L. (1976) Estimating soil moisture in the root zone of crops - a technique adaptable to remote sensing. *Geophys. Res. Lett., 3*, 23-25.

Idso, S.B., Jackson, R.D., and Reginato, R.J. (1975) Estimating evaporation: a technique adaptable to remote sensing. *Science, 189*, 991-92.

Idso, S.B., Schmugge, T.J., Jackson, R.D., and Reginato, R.J. (1975) The utility of surface temperature measurements for the remote sensing of soil water status. *J. of Geophys. Res., 80*, 3044-49.

Idso, S.B., Reginato, R.J., Jackson, R.D., Kimball, B.A., and Nakayama, F.S. (1974) The three stages of drying of a field soil. *Soil Sci. Amer. Proc., 38*(5), 831-37.

Jackson, R.D., Kimball, B.A., Reginato, R.J., and Nakayma, F.S. (1973) Diurnal soil-water evaporation time/depth/flux patterns. *Soil Sci. Soc. Amer. Proc., 37*, 505-9.

Kalma, J.D., and Badham, R. (1972) The radiation balance of a tropical pasture, 1. The reflection of shortwave radiation. *Agric. Meteorol.*, *10*, 251-59.

Kashera, A., and Washington, W.M. (1971) General circulation experiments with a six layer NCAR model, including orography, cloudiness and surface temperature calculations. *J. Atmos. Sci.*, *28*, 657-701.

List, R.J. (1968) *Smithsonian meteorological tables.* 6th Revised Edition, Smithsonian Institute Press, Washington.

Manabe, S., Hahn, D.G., and Holloway, J.L. (1974) The seasonal variation of the tropical circulation as simulated by a global model of the atmosphere. *J. Atmos. Sci.*, *31*, 43-83.

Monin, A.S., and Obukhov, A.M. (1954) Dimensionless characteristics of turbulence in the surface layer. Akad. Nauk. SSSR, Geofiz. Inst. Tr. 24, 163-87.

Monteith, J.L. (1959) The reflection of short wave radiation by vegetation. *Q. J. R. Met. Soc.*, *85*, 386-92.

Monteith, J.L. (1973) *Principles of environmental physics.* Edward Arnold, London.

Moore, D.G., Horton, M.L., Russell, M.J., and Myers, V.I. (1975) Soil moisture and evapotranspiration predictions using Skylab data. Final Report South Dakota State Univ. SDSU-RSL-75-09.

Myers, V.I., Heilman, M.D. (1969) Thermal infrared for soil temperature studies. *Photogrammetric Eng, J.*, 1024-32.

Nakshabandi, G.A., and Kohnke, H. (1965) Thermal conductivity and diffusivity of soils as related to moisture tension and other physical properties. *Agric. Meteorol.*, 2, 1-279.

N.A.S.A. (1978) Heat capability mapping mission data users handbook for application explorer mission A. N.A.S.A., Goddard Space Flight Centre, Greenbelt, Maryland.

N.E.R.C. Report No. GR3/3430 (1978) Newbury Joint Flight Experiment. Paper presented at the Durham Conference of the Remote Sensing Society.

Parks, W.L., Sewell, J.I., Hilty, J.W., Rennie, J.C. (1973) The use of remote multispectral sensing in agriculture. Univ. of Tennessee, Agricultural Experiment Station Bulletin 505.

Paulson, C.A. (1970) The mathematical representation of wind speed and temperature profiles in the unstable atmospheric surface layer. *J. Appl. Meteorol.*, *9*, 857-61.

Philip, J.R. (1966) Plant water relations: some physical aspects. *A. Rev. Pl. Physiol.*, *17*, 245.

Rijtema, P.E. (1965) An analysis of actual evaporation. Agricultural Res. Report No. 659. Centre for Agricultural Publications and Documentation, Wageningen, The Netherlands.

Ripley, E.A. Saugier, B. (1973) Technical report No. 13. Micrometeorology: field data 1971. University of Saskatchewan, Saskatoon, Sask.

Rosema, A. (1975) Simulation of the thermal behaviour of bare soils for remote sensing purposes. In de Vries, D.A., and Afgan, N.H. (Eds.) *Heat and mass transfer in the biosphere.* Scripta Book Co. Washington D.C.

Ross, J. (1975) Radiative transfer in plant communities. In Monteith, J.L. (Ed.) *Vegetation and the Atmosphere, Vol 1. Principles.* Academic Press, London, 13-55.

Sasamori, T. (1970) A numerical study of atmospheric and soil boundary layers. *J. Atmos. Sci, 27*,1122-37.

Sellers, W.A. (1965) *Physical climatology.* Univ. of Chicago Press.

Schmugge, T., Gloeson, P., Wilheit, T., and Geiger, F. (1974) Remote sensing of soil moisture with microwave radiometers. *J. Geophys. Res., 79*(2), 317-23.

Soer, G.J.R. (1977) The Tergra model - a mathematical model for the simulation of the daily behaviour of crop surface temperature and actual evapotranspiration. N.I.W.A.R.S., Publication No. 46, Delft, The Netherlands.

Subbarayuou, J. (1979) Heat capacity mapping mission validation study - final report. Systems and Applied Sciences Corporation.

Tanguay, M.G., Hoffer, R.M., and Miles, R.D. (1969) Multispectral imagery and automatic classification of spectral response for detailed engineering soils mapping. *Proc. 6th Symp. Rem. Sens. of Environ., 1*, 33-63.

Thom, A.S. (1972) Momentum, mass and heat exchange of vegetation. *Quart. J. Roy. Meteorol. Soc., 98*, 124-34.

Thompson, L.M. (1969) Weather and technology in the production of wheat in the U.S. *J. of Soil and Water Conservation, 24*(6), 219-24.

Ulaby, F.T., Cihlar, J., and Moore, R.K. (1973) Active microwave measurement of soil water content. Cres. Tech. Rept. 177-46 to N.A.S.A., University of Kansas.

Waggoner, P.E., Furnival, G.M., and Reifsnyder, W.E. (1969) Simulation of the microclimate in a forest. *Forest Sci., 15*, 37-45.

Watson, K. (1971) A computer program of thermal modelling for interpretation of infrared images. U.S.G.S., Denver, Colorado, GD 71, 023.33p.

Webster, K. (1977) *Quantitative and numerical methods in soil classification and survey.* Clarendon Press, Oxford, pp 269.

Werner, H.D., and Schmer. F.A. (1971) Application of remote sensing techniques to monitoring soil moisture. SO. Dakota, Sta. Univ. Rem. Sens. Inst. Rept. RSI 74-4.

Werner, H.D., and Schmer, F.A. (1972) Application of remote sensing to cropland and rangeland soil water inventory. Final Tech. Repb. SDSU-RSI-72-16, RSI, S. Dakota State Univ.